NON-BOILING HEAT TRANSFER IN HORIZONTAL AND NEAR HORIZONTAL UPWARD INCLINED GAS-LIQUID TWO PHASE FLOW

By

SRINAGA B. KALAPATAPU

Bachelor of Technology

Jawaharlal Nehru Technological University

Hyderabad, India.

2012.

Submitted to the Faculty of the
Graduate College of the
Oklahoma State University
in partial fulfillment of
the requirements for
the Degree of
MASTER OF SCIENCE
July, 2014.

NON-BOILING HEAT TRANSFER IN HORIZONTAL

AND NEAR HORIZONTAL UPWARD INCLINED

GAS-LIQUID TWO PHASE FLOW

Thesis Approved:

Dr. Afshin J. Ghajar

Thesis Adviser

Dr. Khaled Sallam

Dr. AJ Johannes

Name: SRINAGA BHARATH CHANDRA KALAPATAPU

Date of Degree: JULY, 2014

Title of Study: NON-BOILING HEAT TRANSFER IN HORIZONTAL AND NEAR HORIZONTAL UPWARD INCLINED GAS-LIQUID TWO PHASE FLOW

Major Field: MECHANICAL AND AEROSPACE ENGINEERING

ABSTRACT: Heat transfer in non-boiling gas-liquid two phase flow finds its practical application in chemical and petroleum industries. So far, majority of the research dedicated to study heat transfer in non-boiling two phase flow is limited to horizontal and vertical pipe orientations with very little attention given to the study of this phenomenon in inclined systems. To contribute and further enhance the general understanding of heat transfer in non-boiling two phase flow, the main focus of this work is to experimentally measure local and average convective heat transfer coefficients for different flow patterns in horizontal and near horizontal upward inclined two phase flow. In total, 368 experiments are carried out in a 12.5 mm I.D. schedule 10S stainless steel pipe at 0, +5, +10 and +20 degrees pipe orientations using air-water as fluid combination. For each pipe orientation, the superficial gas and liquid Reynolds number is varied from 200 to 19,000 and 2000 to 18,000, respectively and the measured values of the averaged heat transfer coefficient were found to be in a range of 1300 W/m^2K to 8000 W/m^2K. The two phase heat transfer coefficients are compared among the above mentioned orientations. It is found that the two phase heat transfer coefficient increases from 0° to +5° and +10° and then decreases at +20°. Also, correlations in the literature were tested and the best performing correlations have been discussed in the experimental study. Correlation using the concept of Reynolds analogy was developed by modification of the existing correlation in the literature leading towards the better understanding of the relationship of heat transfer phenomenon with the pressure drop.

ACKNOWLEDGEMENTS

I would like to express my deepest gratitude to my adviser Dr. Ghajar, for his immense support, guidance and encouragement throughout my Masters education. His enthusiasm for teaching and dedication in honing young minds is truly inspirational. I am forever indebted to him. I would also express my gratitude to my committee members Dr. AJ Johannes and Dr. Khaled Sallam for their acceptance to be in the committee despite their busy schedules.

I am very much thankful to Mehmat Mollammohtoglu who took his time in training me during my initial days in the lab. A very special thanks to Swanand Bhagwat for being immensely patient during the lab sessions and for his constant cooperation and reliability.

I would like to express my warmest thanks to my friends and lab mates Adekunle Oyewole, Edgar Lares and Tabassum Aziz Hossainy for their constant support and encouragement at all times. I will forever look up to you guys and wish you all the best for your future endeavors.

Last but not the least, this task would have been impossible without the unflinching support of my family, friends and loved ones. I sincerely thank my mother, father, grandfather, grandmother, and my elder brother and loved ones for their immense faith and belief in me. I would like to dedicate this thesis to them for all they have done for me. I dedicate this especially to my father, who has been my friend, guide and my hero since childhood.

TABLE OF CONTENTS

Chapters **Page**

LIST OF TABLES

Table **Page**

LIST OF FIGURES

Figure **Page**

NOMENCLATURE

A	cross sectional area, m^2
C	constant leading coefficient, dimensionless
c	specific heat tat constant pressure, *kJ/kg-K*
c_f	Fanning friction factor, dimensionless
D	diameter of pipe, *m*
D_h	hydraulic diameter, *m*
D_i	inside diameter of pipe, *m*
D_o	outside diameter of pipe, *m*
Eo	Eötvös number, dimensionless
F_p	flow pattern factor, dimensionless
F_s	shape factor, dimensionless
Fr	Froude number (= u^2/gD)
f	constant, dimensionless
f_b	bubble, plug, or slug frequency, s^{-1}
G	mass flux or mass velocity, kg/m^2s
Gr	Grashof number, dimensionless
g	gravitational acceleration, m/s^2
I	intermittent flow

I^*	inclination factor, dimensionless
i	electric current, A
h	heat transfer coefficient, W/m^2K
$\bar{h}$	Circumferentially averaged heat transfer coefficient
K	slip ratio, dimensionless
k	thermal conductivity, $W/m.K$
L	length of test section, m
L_b	bubble, plug, or slug length, m
$\dot{m}$	mass flow rate, kg/s
N_{ST}	no. of thermocouple stations
Nu	Nusselt number ($= hD/k$), dimensionless
Pr	Prandtl number ($= c\mu/k$), dimensionless
p	pressure, Pa
p_a	atmospheric pressure, Pa
$\frac{dp}{dz}$	pressure drop per unit length, Pa/m
Q	volumetric flow rate, m^3/s
$\dot{q}$	heat transfer rate, W
$\dot{q}''$	heat flux, W/m^2
R	electrical resistance, Ω
R_L	liquid fraction or liquid holdup, dimensionless
Re	Reynolds number ($= \rho VD/\mu$), dimensionless
S_L	wetted-perimeter, m
T	temperature, $°C$
ΔT	Temperature drop, ^oC
u	axial velocity, m/s

u_b bubble, plug, or slug velocity, *m/s*

u_{GM} drift velocity, *m/s*

V average velocity, *m/s*

V_D voltage drop, *V*

v specific volume, m^3/kg

w uncertainty, dimension varies with measured parameter

X Martinelli parameter $\sqrt{(\frac{dp}{dz})_{f,SL}/(\frac{dp}{dz})_{f,SG}}$, dimensionless

x flow quality $\dot{m}_G/\dot{m}$, dimensionless;

z Axial direction, *m*

Greek Symbols

α void fraction, dimensionless

μ dynamic viscosity, $N.m/s^2$

ε roughness height of pipe wall, *m*

ν slug frequency in Deshpande et al. (1991) correlation, s^{-1}

ϕ two-phase multipliers, dimensionless

θ inclination angle of pipe or test section, deg. or rad.

ρ density, kg/m^3

σ surface tension, *N/m*

τ_o wall shear stress, N/m^2

Superscripts

m constant exponent, dimensionless

p constant exponent, dimensionless

q constant exponent, dimensionless

r constant exponent, dimensionless

t thermal

Subscripts

ATM atmosphere

avg average

B bulk

btm bottom of the pipe

CAL calculated

eff effective

EXP experimental

f frictional component

G gas phase

i index for *ith* value in mean absolute error equation

in inlet

L liquid phase

out outlet

m mixture

PER peripheral or circmferential

SG superficial gas

SL superficial liquid

SYS system

T top of pipe

TP two-phase

W wall

wi inner wall

wo outer wall

Abbreviations

A	annular
AW	annular wavy
B	bubbly
MabE	mean absolute error (%)
S	slug
SB	slug bubbly
SD	standard deviation
St	stratified
SW	slug wavy
W	wavy
WA	wavy annular

CHAPTER I

INTRODUCTION

Multiphase flow is a type of flow in which different phases of matter move along with each other. Two-phase flow is one such case of multiphase flow. It is the simplest case of multiphase flow which may involve phases of solid-gas, solid-liquid, gas-liquid and two immiscible liquid-liquid combinations. In the current study two phase flow, gas-liquid combination is of interest. Gas-liquid two phase flows have numerous industryial and practical applications. Boiling and non-boiling heat transfer in these phases has caught fascination of the researchers as it has lot of industrial and practical applications. The application of boiling two phase heat transfer is predominant in power plants, nuclear plants, refrigeration plants and air conditioning plants. Non-boiling heat transfer is more predominant in oil and natural gas industry, process industry and also in processes that involve mass transfer in chemical industries.

The basic step in understanding any heat transfer process of a two phase flow is identifying and classifying flow pattern. In thermal hydraulics determination of flow pattern has been a problem. This is because the flow pattern or the flow regime of a flow is usually subjective and no proper tool exists to determine it. Some flow patterns are favorable in some cases and applications while other flow patterns are totally undesirable in industries. For instance, slug formation during the transport of oil by water or gas is not favorable to the receiving facilities at the outlet. The slug formation during the oil transport severely decreases the discharge of oil at the outlet. Water and

oil tend to form emulsions thereby increasing the pressure drop and decreasing the production. In chemical industries the presence of water slugs in the oil leads to the corrosion of the pipe damaging the pipe and transport system.

So, two phase flow regime identification methodologies are important and proper methodology should be developed in identifying and classifying the flow pattern. Julia et al. (2009) developed these methodologies introducing techniques of neural networks in classifying the flow regimes. Flow patterns for different flow rates have been identified using conductivity probes and signal detection. The presence and the movement of bubbles, elongated bubbles and slugs formed during the flow are measured by the lapse in time. This signal detection is further processed using statistical tools of probability distribution functions to correctly identify the flow pattern. The flow pattern identified is further classified into different flow regimes and the transition boundaries are drawn based on employing the tool of neural networks. This flow regime identification and classification will give a proper insight in understanding the flow pattern of the flow for particular flow rates. In thermal hydraulic applications this classification leaves a blueprint for the user to operate in desired flow rate/flow pattern.

In power generation, boiling two phase flow is always present and the phenomenon plays an important role in the performance of the generation unit. In automobiles boiling two phase is usually seen in the power house of an automobile, the engine. The lifespan of an engine is usually determined by its thermal loading. To cool the engine's cylinder head from excessive heating due to combustion water-glycol (50%-50%) is pumped through the cavities and channels. Due to high local heat fluxes nucleate boiling occurs near the cylinder flame deck. Kroes et al. (2009) modelled the system of engine cylinder and analyzed the bubble formation and suppression due to the boiling. The enhancement of the heat transfer is observed due to bubble sliding and formation and also due to forced convection. Several techniques have been developed and the development is still in progress for effective cooling using two-phase mixtures and cooling phenomenon.

The two phase enhancement of heat transfer observed during the process of cooling also finds its place in space application. In conventional space applications, the increase in area space platforms resulted in increased wastage of heat generated which flows to radiator and to the cold of space. Till date, conventional single phase heat transfer loops have been used for spacecraft's active thermal control. The impact of two-phase heat transfer in low gravity applications is studied by DiMarco et al. (2009) and explains the advantages of using two phase heat transfer in low gravity. In low gravity atmospheres heat removal by the flow of single phase liquid is based on the sensible heat of the liquid. But in fluids heat exchange can also take place through latent heat at a constant temperature with change of phase. Boiling is recognized as an effective technique in removing large amounts of heat at low temperatures. This technique can be adopted to space gravity thereby reducing the fluid flow for better thermal control and reduction in wastage of energy and pumping power. DiMarco et al. (2009) discuss the further research plan in the field showing the development of two phase flow even in space based applications.

Two phase flow heat transfer is also a phenomenon seen in refrigeration and heat exchangers as boiling and condensation are extensively involved. Sardeshpande and Ranade (2013) review the literature in two phase boiling in small channels. Since the past 50 years, the research in two phase flow heat transfer ranging from small, mini and micro channels and compact heat exchangers shows the ongoing research in two phase flow heat transfer.

The non-boiling heat transfer in oil industry focuses on the problems of transporting oil and natural gas in pipes at different orientations. Ongoing research to understand the flow behavior and heat transfer characteristics in two phase flow for different pipe materials, different diameters and different inclinations is of interest to the researchers and the industry alike.

In oil industry, the temperature of the hydrocarbon fluids flowing in the pipe during transportation changes due to the difference in temperature of the surface and the oil reservoir. This results in wax

deposition in the inner walls of the pipe blocking fluid flow thereby causing severe mechanical problems. This wax deposition has been reportedly said to cause economic losses along with mechanical problems. A direct cost of 5 million dollars to remove a blockage caused by wax deposition from a subsea pipeline with production downtime loss of 40 days and 25 million dollars has been reported Fogler (2008). A British company named Lasmo Company abandoned an oil platform amounting to loss of 100 million dollars has also been reported by Singh et al. (2000).

The current study focuses on the non-boiling two phase heat transfer involving gas-liquid flows. Air-water flow in horizontal and upward inclined pipes is studied in the current experiment.

1.1 Basic Definitions of a Two-Phase Flow

Two phase flow is a much more complicated phenomenon than single phase flow. The interaction of gas-liquid with each other flowing through a pipe makes the two phase flow difficult to model and understand mathematically and physically than the single phase flow. Two phase flow depends on several factors like nature of the gas, nature of liquid and pipe materials. By varying parameters like pipe diameter, pipe length and gas-liquid flow rate the physics of the flow is greatly affected. This poses certain complexities in the analyzing the two phase flow. The problem becomes much more complex while analyzing 3-D transient flow in a pipe. The definitions present here are that of one dimensional flow and are most prevalent in developing and analyzing two-phase pressure drop, void fraction and heat transfer.

The total mass flow rate ($\dot{m}$) through the tube is equal to the sum of the mass flow rates of gas ($\dot{m}_G$) and liquid ($\dot{m}_L$):

$$\dot{m} = \dot{m}_G + \dot{m}_L \tag{1.1}$$

The flow quality (x), which is the ratio of the gas mass flow rate to the total mass flow rate is defined as

$$x = \frac{\dot{m}_G}{\dot{m}} = 1 - \frac{\dot{m}_L}{\dot{m}} \tag{1.2}$$

The mass flux (G) or the mass velocity is defined as

$$G = \frac{\dot{m}}{A} \tag{1.3}$$

where the total cross sectional area (A) is the total cross sectional areas occupied by both gas and liquid phases defined as $A = A_G + A_L$.

Void fraction (α) is defined as the volume of the space occupied by as gas phase in a two phase flow in pipe/tube, hence for the total cross section area of the pipe A, the void fraction can be defined by

$$\alpha = \frac{A_G}{A} \tag{1.4}$$

and the liquid hold up is given by

$$R_L = 1 - \alpha = \frac{A_L}{A} \tag{1.5}$$

Many models were developed to understand the two-phase flow. Drift flux model is one of them, where the two phase flow is studied based on the superficial velocities of the liquid and gas. Many correlations use superficial velocities for the analysis of two-phase flow. Superficial velocity is the velocity of the liquid or gas phase would exhibit if it would flow alone in the tube without another phase. The superficial gas velocity in a pipe (u_{SG}) is given by

$$u_{SG} = \frac{Gx}{\rho_G} = \frac{Q_G}{A} \tag{1.6}$$

The actual gas velocity can be expressed by

$$u_G = \frac{Q_G}{\alpha A} \tag{1.7}$$

Similarly, superficial liquid velocity (u_{SL}) is expressed as

$$u_{SL} = \frac{G(1-x)}{\rho_L} = \frac{Q_L}{A} \tag{1.8}$$

The actual gas velocity can be expressed by

$$u_L = \frac{Q_L}{(1-\alpha)A} \tag{1.9}$$

The slip ratio (*K*) is defined as the ratio of the actual velocities between the phases, which can be expressed as follows

$$K = \frac{u_G}{u_L} = \left(\frac{x}{1-x}\right)\left(\frac{\alpha}{1-\alpha}\right)\frac{\rho_L}{\rho_G} \tag{1.10}$$

When the velocity of the gas phase is equal to the velocity of the liquid phase, then $K = 1$ and there is no slip between the gases. This no-slip condition between the two phases is called homogenous two phase flow.

Two phase flow requires the expressions of few standard properties like density and viscosity. This becomes important as most of the correlations in two-phase flow use the fundamental two phase properties in defining some of the other flow parameters or characteristics. The flow physics of the two phase flow is explained by understanding the behavior of gas and liquid phase independently and their interaction in a tube. So two phase parameters are essentially defined.

The two phase density (ρ_{TP}) is expressed as

$$\rho_{TP} = \rho_L (1-\alpha) + \rho_G \alpha \tag{1.11}$$

The two phase viscosity (μ_{TP}) is defined as

$$\mu_{TP} = \mu_L (1-\alpha) + \mu_G \alpha \tag{1.12}$$

Reynolds number is one of the most important dimensionless numbers in fluid mechanics and dynamics. In two phase flow it can be defined in many ways. But, one of the most prevalent way of defining Reynolds number is through superficial Reynolds number. The superficial gas Reynolds number (Re_{SG}) is defined as follows

$$\mathrm{Re}_{SG} = \frac{\rho_G u_{SG} D}{\mu_G} = \frac{xGD}{\mu_G} \tag{1.13}$$

The superficial liquid Reynolds number (Re_{SL}) is given by

$$\mathrm{Re}_{SL} = \frac{\rho_L u_{SL} D}{\mu_L} = \frac{(1-x)GD}{\mu_L} \tag{1.14}$$

In some cases, in situ Reynolds liquid phase number (Re_L) preferred over the superficial liquid Reynolds number (Re_{SL}). In such cases, the in situ liquid Reynolds number is given by

$$\mathrm{Re}_L = \frac{\rho_L u_L D_L}{\mu_L} = \frac{4\dot{m}_L}{\pi\sqrt{(1-\alpha)}\mu_L D} \tag{1.15}$$

1.2 Basic Flow Phase Flow Patterns

The gas and liquid phases exist in different morphological shapes. The basic shapes in which they exist can be classified as a flow pattern. Some basic flow patterns were observed by the researchers and their flow physics has been studied. Flow pattern is very important as they strongly dictate the hydrodynamics of the flow in a two phase flow. Pressure drop, void fraction and heat transfer are greatly influenced by flow patterns.

Flow pattern in two phase horizontal orientation

The basic flow patterns in a horizontal tube with circular cross section are shown in **Figure 1.1**. One of the important features observed in the horizontal flows is the flow stratification of the flow. The stratified flow observed in the horizontal flow disappears in the upward inclination flows but is observed in the downward inclined tubes. Though, intermittent flows are observed traversing the transitional boundaries of flow pattern in a flow map, we define common observed flow patterns in horizontal orientation in the section.

Bubbly flow: This type of flow is observed at very low quality. Due to buoyancy the bubbles usually stay on the top surface of the pipe and flow at the upper portion of the pipe.

Plug flow: This type of flow is observed when the bubbles of small size coalesce to form bubbles of plug shape. Subjectively this plug flow may sometimes be defined as slug flow or elongated bubbly flow.

Stratified flow: At very low liquid and gas flow rates, stratified flow is observed. Due to gravitational forces the liquid layer stays at the bottom and the gas layer flows at the top clearly showing the distinction between gas and liquid flows.

Wavy flow: When the gas flow rate is increased in the stratified flow, it creates a disturbance and forms waves in the flow. These disturbances result in the formation of waves terming it as a wavy flow.

Slug flow: Slug flow is characterized by the large bubbles almost filling the entire tube. These large U shaped bubbles are called Taylor bubbles or slugs. This type of flow is called the slug flow where lot of research is currently in progress.

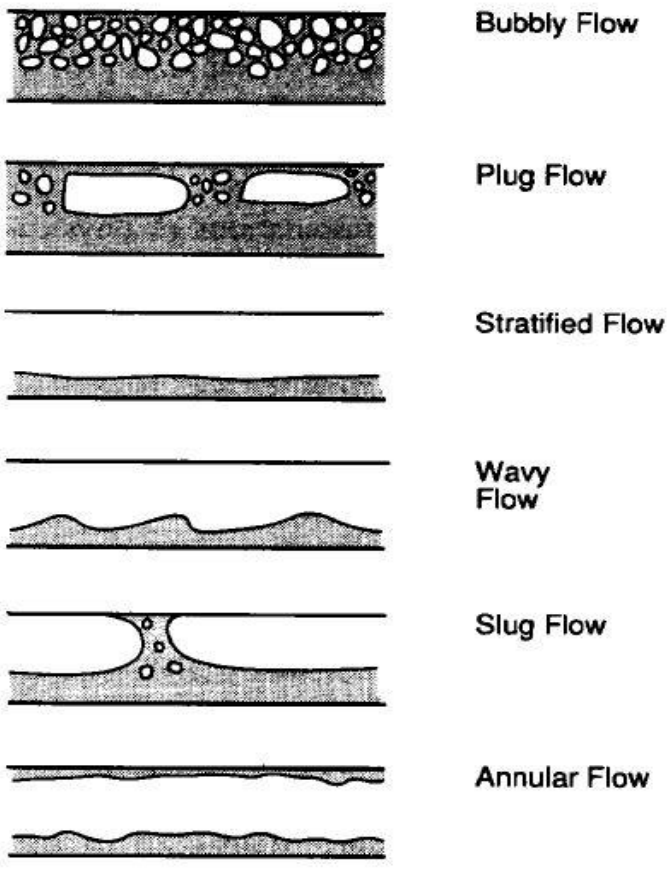

Figure 1.1 Schematic of flow patterns observed in horizontal gas-liquid flow (from Carey (1992))

Annular flow: Annular flow consists of gas core wrapped inside a liquid film or vice versa observed in high liquid and gas flow rates.

1.3 Research Objectives

The main objective of the research is to establish the effect of heat transfer in upward inclined orientations in a non-boiling two phase air-water pipe flow. Due to the lack of literature regarding flow regimes and thermo-fluid dynamics in inclined pipes, experimental work in this study is carried to fill the gap in literature and enhance understanding of the two phase heat transfer phenomenon in inclined non-boiling systems. Parameters like flow pattern, void fraction and pressure drop along with pipe orientation influence the heat transfer in a pipe. In the current research we observe the effect of flow pattern and pipe inclination on the heat transfer of the two phase flow. This gives a greater insight into fundamental understanding of the heat transfer phenomenon. The qualitative understanding fetched by collecting the data through heat transfer experiments can be used for understanding the phenomenon quantitatively by forming correlations or by testing the robustness of the existing correlations with the data. The current experiments performed answers the following questions:

1) What is the effect of flow pattern on heat transfer coefficient?
2) What is the effect of pipe inclination on heat transfer coefficient?
3) What is the best performing heat transfer correlation in the upward inclination?
4) Can a possible Reynolds analogy be developed for the heat transfer experimental data?

The study undertaken is divided into parts to properly understand the effect of heat transfer in upward inclinations.

- Literature search on the available literature on two-phase flow heat transfer involving the effects of flow pattern and inclination studying the methodologies and experimental data.

- Heat transfer data has been collected involving the orientations of 0°, +5°, +10° and +20°
- The heat transfer data was analyzed to find the variables and parameters that affect the heat transfer coefficient.
- Correlations are tested for current experimental data and the best performing correlations have been reported.
- Exploring the viability of Reynolds analogy correlation with the help of experimental data.
- Documenting and presenting the research findings in the form of Master's thesis as deliverables.

1.4 Brief Outline of the Study

The contents in the manuscript are geared towards the study and research of non-boiling two phase flow. Chapter II focuses on the review of selected literature of two phase flow in heat transfer in horizontal, upward inclined and other orientations. The chapter also includes selected research on Reynolds analogy literature. Chapter III details the experimental setup, apparatus and methodology of the experimental procedure. Also, validation of the experimental setup with uncertainty is explained in the chapter. Chapter IV discusses the results in detail addressing the questions and finally Chapter V summarizes the study with concluding remarks and recommendation for future studies.

CHAPTER II

LITERATURE REVIEW

Several investigators have studied the literature in two phase flow. Several correlations were developed taking flow parameters into account. Broadly, the available heat transfer correlations in the literature comprising of horizontal and near horizontal inclination flows can be divided into two classes' viz. general heat transfer correlations and Reynolds analogy correlations.

The general heat transfer correlations are developed based on the dependence of *k, c, u, μ, ρ* and *D*. Typically, these correlations are developed like the single phase heat transfer correlations involving parameters like

$$Nu = hD/k \tag{2.1}$$

$$\mathrm{Re} = \mu Du/\rho \tag{2.2}$$

$$\mathrm{Pr} = \mu c/k \tag{2.3}$$

Using Buckingham pi theory, the above dimensionless numbers have been developed and the functional dependence of the above dimension less numbers has been given by

$$Nu = f(\mathrm{Re}, \mathrm{Pr}) \tag{2.4}$$

The function in Equation (2.4) forms the basis for single phase/two phase correlations shown as

$$Nu = {hD}/{k} = C\,\mathrm{Re}^{a}\,\mathrm{Pr}^{b} \qquad \text{or} \qquad h = C\,\mathrm{Re}^{a}\,\mathrm{Pr}^{b} \tag{2.5}$$

where *C*, *a* and *b* are experimentally determined constants.

Understanding the correlations and experimental methodology developed by the investigators forms a basis for the current experiment. Some observations made by the previous researchers have also been observed in the current research. The chronological order of the literature review also helps in understanding the development of the research in the field.

2.1 General Two Phase Heat Transfer Literature

Knott et al. (1959) conducted experiments on two phase flow involving mixtures of viscous oil and nitrogen. The authors observed the increase of two phase transfer heat transfer coefficient involving liquid-gas mixture when opposed to single phase flow. In the bubbly flow regime, the authors observed increase of two phase heat transfer coefficient for same liquid discharge as in single phase due to the increase of overall gas phase discharge. Based on the observations, the authors suggested the following two phase heat transfer correlation involving mean velocities of gas and liquid.

$$\frac{h_{TP}}{h_L} = \left(1 + \frac{u_{SG}}{u_{SL}}\right)^{\frac{1}{3}} \tag{2.6}$$

where h_L is determined from Sieder and Tate (1936) equation.

Knott et al. (1959) correlation is found to perform considerably well even in near horizontal inclinations involving upward and downward orientations. Current experimental data populated

involving orientations of 0, +5°, +10° and +20° found Knott's correlation one of the best performing correlations.

Oliver and Wright (1964) performed experiments on gas-liquid two phase flows exclusively focusing on slug flow regime. The study was conducted in horizontal tubes with a diameter of 12.7 *mm*. with Newtonian and non-Newtonian fluids. Higher heat transfer was observed in two-phase slug flow when compared to single phase especially in the void fraction rage of 0.5 - 0.8. While developing their correlations, the authors assumed that there is no slip between the two-phases and liquid phase is dominating heat transfer and flow characteristics. The proposed heat transfer correlation for Newtonian fluids is given by

$$Nu_{TP} = Nu_L \left(\frac{1.2}{R_L^{0.36}} - \frac{0.2}{R_L} \right) \tag{2.7}$$

where Nu_L is determined by

$$Nu_L = 1.615 \left[\frac{(Q_G + Q_L)\rho D}{A\mu} \mathrm{Pr}_L \frac{D}{L} \right]^{\frac{1}{3}} \left(\frac{\mu_B}{\mu_W} \right)^{0.14}$$

Hughmark (1965) developed correlations for two phase gas-liquid slug and bubbly region hold-up and heat transfer in horizontal flow. Two correlations were developed based on two models for slug flow heat transfer. For laminar flow, correlation based on Graetz-Leveque equation is suggested and for turbulent flow correlation based on momentum-turbulent analogy is suggested. For turbulent flow, the slug liquid Reynolds number range was from 26,000 to 4.5×10^6. The maximum Reynolds number for the current experiment in the slug flow does not exceed 10,000. For laminar slug flow, Hughmark (1965) proposes the following correlation

$$Nu_{TP} = 1.75 R_L^{-0.5} \left(\frac{\dot{m}_L c_L}{R_L k_L L} \right)^{\frac{1}{3}} \left(\frac{\mu_B}{\mu_W} \right)^{0.14} \tag{2.8}$$

The liquid slug Reynolds number range for the proposed correlation was from 1600 to 4600.

Martin and Sims (1971) studied two phase flow forced convection in water with air injected in a rectangular duct. The experimental test section consisted of a horizontal rectangular channel with inner cross section of the dimensions 0.52 × 0.257 *in.* with 0.52 *in.* vertical wall. At the bottom of the channel a heated porous element was present 0.0365 *in.* thick and 0.257 *in.* wide for the passage of air. This system enabled the authors to observe every flow pattern from slug flow to annular progressively and with increase in superficial gas velocity, the authors observed an increase in heat transfer coefficient. The main dependent variables were heat transfer coefficient and flow pattern, while the independent variables were air injection and superficial velocities of gas and liquids. The proposed correlation by Martin and Sims (1971) can be expressed as

$$\frac{h_{TP}}{h_L} = 1 + 0.064\left(\frac{u_{SG}}{u_{SL}}\right)^{0.5} \tag{2.9}$$

where h_L is determined by Sieder and Tate (1936) equation. The correlation was said to predict 88% of the measured data with 52 points within range of ±20%. Also, the study was conducted by the authors in rectangular channels, it is to be noted that the data cannot be replicated for circular tubes.

Shah (1981) worked with around 670 data points in horizontal and vertical channels with circular and non-circular tubes. The experimental analysis compiled the data that consisted of 10 liquid-gas mixture combinations, hydrodynamic diameter ranging from 4 to 70 *mm* and a wide range of heat and mass flux. The correlations developed by Shah (1981) predicted 96% of the data within the range of ±30% error and had a root mean square error of 15.5%. The correlation proposed by Shah (1981) is given by

$$\frac{h_{TP}}{h_L} = \left(1 + \frac{u_{SG}}{u_{SL}}\right)^{0.25}, \qquad (\text{for } \mathrm{Re}_{SL} < 170) \tag{2.10}$$

where

$$Nu_L = 1.86\left[\mathrm{Re}_{SL}\,\mathrm{Pr}_L\left(D/L\right)\right]^{\frac{1}{3}}\left(\mu_B/\mu_W\right)^{0.14} \tag{2.11}$$

For Re_{SL} > 170, Shah (1981) gives a graphical correlation stating that it is difficult to express mathematically. The data populated in the current experiment too shows good agreement with the Shah (1981) correlation which was shown above for the Re_{SL} > 170 . Shah (1981) correlation is the best correlation for current experimental data involving horizontal and near horizontal upward inclinations.

Shoham et al. (1982) conducted experiments on two phase gas-liquid slug flow in horizontal orientation. The experimental setup consisted of 3.81 *cm* I.D. by 6.35 *cm* O.D. brass pipe with 176 *cm* length heated with the help of electrical elements passing uniform heat flux. The experimental setup facilitates for the circumferential arrangement of the thermocouples to calculate the heat transfer coefficient. The liquid water flow rates ranged from (0.45 – 1.59) × 10^{-2} *kg/s* and the gas flow rates ranged from (0.23 – 1.09) × 10^{-2} *kg/s*. The authors observed that the bottom surface of the pipe which was consistently in contact with the liquid phase has a higher heat transfer coefficient than the top surface which is constantly in touch with the gas surface by at least a factor of 2. They have also observed that the liquid phase is dominant in affecting the heat transfer characteristics. The ratio of top and bottom surface of the Nusselt number Nu_{top}/Nu_{bottom} was found to be less for high liquid low gas flow rate. When the liquid flow rate is constant, the ratio Nu_{top}/Nu_{bottom} is found to be increased with increasing gas flow rate.

Drucker et al. (1984) studied the single and two component, two phase heat transfer mechanisms for vertical flow inside the tubes with blockages. Reynolds number with a range of 2000 to 150,000 and void fractions up to 0.40. The authors found that there was a significant increase in the heat transfer coefficient in the downstream. The proposed correlation is as follows

$$\frac{h_{TP}}{h_L} = 1 + 2.5\left(\alpha Gr / \mathrm{Re}_{TP}^2\right)^{0.5}$$
$$Gr = \left[\left(\rho_L - \rho_g\right) g D^3\right] \Big/ \rho_L \nu_L^2 \tag{2.12}$$

Deshpande et al. (1991) conducted experiments on horizontal slug-plug flows in two phase air-water mixture electrically heated. Stainless steel pipes of diameters 0.028 *m* and 0.057 *m* inside diameters were employed for the study. The water velocity ranged from 0.2 - 1.11 *m/s* and the air velocity ranged till 3.6 *m/s*. Axially placed thermocouples record the temperatures and are used to measure the time averaged heat transfer coefficient at the top and bottom surfaces. Slug length, slug frequency, mixture velocity were found to be important factors that affect the heat transfer coefficient. They have observed the decrease of heat transfer coefficient in the top surface when compared to top surface due to the presence of liquid in the bottom surface. This observation is consistent with that made by Shoham et al. (1982). The increase of slug frequency with the increase of superficial liquid velocity (u_{SL}) decreased the ratio of the heat transfer coefficients between the top and bottom surface ($h_{TP,\,top}$ / $h_{TP,\,btm}$). Correlations were presented by the authors to determine $h_{TP,\,top}$, $h_{TP,\,btm}$, and $h_{TP,\,avg}$. Around 94% of the points for $h_{TP,\,btm}$, and $h_{TP,\,avg}$ of the experimental data were predicted within ±10% range and 90% of the points for $h_{TP,\,top}$ within ±15% error. The correlation given by Deshpande et al. (1991) is as follows

$$Nu_{TP,\mathrm{btm}} = 0.023\,\mathrm{Re}_L^{\,0.83}\,\mathrm{Pr}_L^{0.4}\left(\frac{u_{SL}}{u_m} - 0.1\right)^{0.3} \tag{2.13}$$

$$Nu_{TP,\mathrm{top}} = 1.93\,\mathrm{Re}_m^{\,0.44}\,\mathrm{Pr}_m^{0.4}\left(\frac{u_{SL}}{u_m}\right)^{0.21}\left(\frac{u_{SL}\nu}{g}\right)^{0.53} \tag{2.14}$$

where

$$\mathrm{Re}_L = \frac{Du_m\rho_L}{\mu_L}; \quad \mathrm{Re}_L = \frac{Du_m\rho_m}{\mu_m}; \quad u_m = u_{SL} + u_{SG};$$

$$\nu = 0.0434\left[\left(\frac{u_{SL}}{u_m}\right)\left(\frac{2.02}{D} + \frac{u_m^2}{gD}\right)\right]^{1.02}$$

Hetsroni et al. (1998a,b) studied on two phase horizontal and near horizontal inclinations like +2° and +5° mostly on slug and plug flow. They conducted experiments on heated test section with inner diameter of 49.2 *mm* and *L/D* ratio of 3.6 which is electrically heated. The thermal profiles are observed using an infrared thermograph at *L/D* = 0.45, 0.9 and 2.4. The parameters that influenced the heat transfer coefficient at the top surface were superficial liquid velocity (u_{SL}), bubble length (L_b), bubble velocity (u_b) and bubble frequency (f_b). The authors also observed that the heat transfer coefficient increased with the increase in inclination in near horizontal orientations. The correlation proposed by Hestroni et.al (1998a, b) can be expressed as

$$h_{TP} = 0.15\left(h_{TP}\right)_{\varphi} + 0.85h_L \qquad \begin{array}{l}\varphi < 0.3 \\ \text{for } 0.9 < Fr_L < 2.0 \\ 0.03 < Fr_G < 0.43\end{array} \qquad (2.15)$$

where h_{TP} and h_L are determined using

$$\left(h_{TP}\right)_{\varphi} = h_L\left[0.40 + 0.54Fr_L^{1.2}\exp\left(-\frac{f_b L_b}{u_b}\right)\right]$$

$$Nu_L = 0.0155\,\mathrm{Re}_L^{0.83}\,\mathrm{Pr}_L^{0.5}$$

Kim (2000) conducted an extensive survey of 20 correlations in which most of them involved correlations for vertical flow. Most of the correlations tabulated by Kim are tabulated in **Table 2.1** along with some important and better performing correlations for horizontal and also inclined flows for the current experimental data.

Kim et al. (2000) developed a correlation to predict the non-boiling two phase heat transfer rate regardless flow pattern, pipe orientation and pipe inclination. The correlation proposed based on turbulent flow Re_{SL} > 4000 in vertical orientation with different flow patterns and combinations. 255 experimental data points from the literature have been used to determine the constants in the proposed correlation. The correlation successfully predicted the overall absolute mean deviation for about 2.5% and an rms deviation about 12.8%. The proposed correlation also predicted about 83% error in ±15% deviation and 96% of the data within ±30% of deviation. The proposed correlation is as follows

$$h_{TP} = (1-\alpha) h_L \left\{ 1 + C \left[\left(\frac{x}{1-x} \right)^m \left(\frac{\alpha}{1-\alpha} \right)^n \left(\frac{\mathrm{Pr}_G}{\mathrm{Pr}_L} \right)^p \left(\frac{\mu_G}{\mu_L} \right)^q \right] \right\} \tag{2.16}$$

The constant values used to analyze the data in the current experiment has also been proposed and the correlation used in the current experiment is

$$h_{TP} = (1-\alpha) h_L \left\{ 1 + 0.27 \left[\left(\frac{x}{1-x} \right)^{-0.04} \left(\frac{\alpha}{1-\alpha} \right)^{1.21} \left(\frac{\mathrm{Pr}_G}{\mathrm{Pr}_L} \right)^{0.66} \left(\frac{\mu_G}{\mu_L} \right)^{-0.72} \right] \right\} \tag{2.17}$$

Kim and Ghajar (2006) developed correlations based on 408 experimental data points covering different flow patterns, flow combinations and spanning through orientations 0°, 2°, +5°, and 7°. To account for the flow pattern and inclination characteristics the authors introduced flow pattern factor (F_P) and inclination factor (I). This correlation successfully predicted 90% of the data within ±20% agreement. The correlation given by the authors is

$$h_{TP} = F_P h_L \left\{ 1 + C \left[\left(\frac{x}{1-x} \right)^m \left(\frac{1-F_P}{F_P} \right)^n \left(\frac{\mathrm{Pr}_G}{\mathrm{Pr}_L} \right)^p \left(\frac{\mu_G}{\mu_L} \right)^q \right] (I)^r \right\} \tag{2.18}$$

where h_L is determined by Sieder and Tate (1936) equation and *m, n, p, q* and *r* are adjustable constants.

Tang and Ghajar (2011) conducted extensive research in non-boiling two phase heat transfer by studying 38 correlations in all orientations that have been published in the literature in the past 50 years of non-boiling two phase flow research. The authors performed experiments in horizontal and near horizontal orientations of +2°, +5° and +7° spanning different flow patterns and different fluid combinations. Flow patterns and flow maps were drawn for the said inclinations so as to understand the impact of flow pattern and its extent with inclination in two-phase non-boiling heat transfer. A total of 986 experimental points have been populated in different orientations and the correlations were compared against the data. The authors observed that the heat transfer coefficient increased with the increase in orientation to a certain extent (in this case up to 7°) are predicted that with increase in inclination may not increase the heat transfer coefficient which is found to be evident with the data populated in current experiment. The authors conducted the experiments consisting a test section with straight standard stainless steel schedule 10S pipe with 27.9 *mm* I.D. and *L/D* ratio of 95 supplied with a uniform heat flux by Lincoln SA-750 welder. The correlation suggested by follows that of Equation (2.18) which includes modified inclination factor (I^*) taking care of many inclinations and flow patterns.

$$h_{TP} = F_P h_L \left\{ 1 + 0.55 \left[\left(\frac{x}{1-x} \right)^{0.1} \left(\frac{1-F_P}{F_P} \right)^{0.4} \left(\frac{\mathrm{Pr}_G}{\mathrm{Pr}_L} \right)^{0.25} \left(\frac{\mu_G}{\mu_L} \right)^{0.25} \right] \left(I^* \right)^{0.25} \right\} \tag{2.19}$$

$$F_P = (1-\alpha) + \alpha F_S^2; \qquad F_S = \frac{2}{\pi} \tan^{-1} \left(\sqrt{\frac{\rho_G \left(V_G - V_L \right)^2}{gD\left(\rho_L - \rho_G \right)}} \right)$$

$$I^* = 1 + Eo\left|\sin\theta\right|; \qquad Eo = \frac{\left(\rho_L - \rho_G \right) gD^2}{\sigma}$$

where h_L is determined by Sieder and Tate (1936) equation andt α is determined by Woldesemayat and Ghajar (2007)

The correlations and the experimental procedures performed the investigators in two-phase flow gives a better picture in understanding the development of the subject so far and its evolution in the

future. The literature review thus provides a guideline for the current and future researchers to fill the gaps that are present.

2.2 Reynolds Analogy and Other Literature

Reynolds analogy is relating momentum transfer with heat transfer. This kind of expressing momentum transfer with heat transfer is called Reynolds analogy. This is done due to the fact that there a practical limitations in measuring heat transfer in two phase flow. But, investigators like King (1952) and Vijay et al. (1982) attempted to express heat transfer based on pressure drop or momentum data. In the current experimental analysis, Vijay et al. (1982) correlation is modified to mechanistically relate heat transfer to momentum transfer which is discussed in Chapter 4.4. The general formation of Reynolds analogy can be shown as follows involving dimensionless parameters like Nusselt number (*Nu*), Reynolds number (Re) and Prandtl Number (Pr).

$$\frac{c_f}{2} = Nu\left(\mathrm{Re}\,\mathrm{Pr}\right)^{-1} \tag{2.20}$$

For the flow inside the pipes with frictional pressure gradient

$$\left(-\frac{dp}{dz}\right)_f = \frac{4\tau_0}{D} = \frac{2c_f}{D\rho}\left(\frac{\dot{m}}{A}\right)^2 \tag{2.21}$$

Combining the equations (2.20) and (2.21), and adopting the definitions of *Nu*, Re and Pr we end up with expression

$$h = \frac{\rho c}{\dot{m}}\left(-\frac{dp}{dz}\right)_f \frac{A^2}{\pi D} \tag{2.22}$$

Using equation (2.22) to define heat transfer coefficient for two phase flow Reynolds analogy form of the two phase flow can be obtained as follows

$$\frac{h_{TP}}{h_L} = C\frac{\dot{m}_L}{\dot{m}}\frac{\rho_{TP}}{\rho_L}\frac{\left|dp/dz\right|_{f,TP}}{\left|dp/dz\right|_{f,L}} = C\frac{\dot{m}_L}{\dot{m}}\frac{\rho_{TP}}{\rho_L}\phi^2 \tag{2.23}$$

Here, C would be determined experimentally involving certain hydrodynamic and flow and parameters. Φ^2 is recognized as the pressure drop multiplier defined by **Lockhart and Martinelli (1949)**.

Johnson and Abou-Sabe (1952) performed heat transfer and static pressure drop experiments in a horizontal brass tube with 25.4 *mm* I.D. and length 4.57 *m.* The liquid flow rate ranged from 7.56 to 113 *kg/min* and the gas flow rate ranged from 0 to 1.51 *kg/min* of air. The air-water mixture test section was heated with uniform wall temperature and the authors observed an increase in heat transfer coefficient when compared to single phase. A correlation was suggested by the authors whose data spanned different flow patterns in a horizontal tube. The correlation is expressed as

$$\frac{h_{TP}}{h_L} = \frac{R_L^{-0.5}}{1+0.006\,\mathrm{Re}_{SG}^{0.5}}\left(\phi_L^2\right)^{0.3333} \tag{2.24}$$

where h_L is determined by $Nu_L = 0.023\,\mathrm{Re}^{0.8}\,\mathrm{Pr}^{0.4}$

King (1952) performed experiments in a horizontal copper tube with I.D. of 18.7 *mm*. Pressure drop and heat transfer experiments performed by King led to similar conclusions as **Johnson and Abou-Sabe (1952).** Also King (1952) modified the correlation by Abou-Sabe (1952). The correlation of King is given by

$$\frac{h_{TP}}{h_L} = \frac{R_L^{-0.52}}{1+0.006\,\mathrm{Re}_{SG}^{0.5}}\left(\phi_L^2\right)^{0.32} \tag{2.25}$$

where h_L is determined by $Nu_L = 0.023\,\mathrm{Re}^{0.8}\,\mathrm{Pr}^{0.4}$

Aggour (1978) performed two phase experiments on a two phase heat transfer in vertical inclination using air-water, helium-water and Freon 12-water mixtures. The heat transfer test section consisted of 0.46 *in.* of I.D. tube with 2 *ft* in length. Alternating current is used for heating the test section. A correlation has been developed with experimental data points collected with Re_{SL}

ranging from 265 to 4090 and Re_{SG} 48 to 16,265. The authors found that for same gas and liquid flow rates, the heat transfer coefficient increases with the increase in density of the gas. From the 50 data points collected in Helium-water 92% of the points lie within ±30% and among the 44 data points collected in Freon 12-water 86% of the data lies with ±30%. Also, excellent agreement is shown while the correlation is tested for other data points available in the literature with a mean deviation of 7.2% and rms deviation of 30.7% for 2142 data points predicting 93% of them within the range of ±50%. The correlation predicted by the author is as follows

$$
\begin{aligned}
&h_{TP}/h_L = (1-\alpha)^{-\frac{1}{3}} && \text{(L)}\\
&\text{where } Nu_L = 1.615\left[\mathrm{Re}_{SL}\,\mathrm{Pr}_L\,(D/L)\right]^{\frac{1}{3}}\left(\frac{\mu_B}{\mu_W}\right)^{0.14} && \text{(L)}\\
&h_{TP}/h_L = (1-\alpha)^{-0.83} && \text{(T)}\\
&\text{where } Nu_L = 0.0155\,\mathrm{Re}_{SL}^{0.83}\,\mathrm{Pr}_L^{0.5}\left(\frac{\mu_B}{\mu_W}\right)^{0.33} && \text{(T)}
\end{aligned}
\qquad (2.26)
$$

Ravipudi and Godbold (1978) studied the effect of mass transfer rates on heat transfer rate and coefficient in two phase flow. Unsurprisingly, it was found that as the mass transfer rate from liquid to gas increases, the heat transfer rates increase but the heat transfer coefficient decrease. This was attributed to the fact that the dependence of the heat transfer coefficient with mass transfer was a function liquid and gas mass flux densities, vapor pressure of the liquid and total pressure of the system. With high mass transfer rates, the heat transfer to the two phase mixture steam condenser was transferred to the humidified air leaving system. But, the heat transfer coefficient was found to increase with a constant mass transfer rate in a two phase flow and a correlation was formed by the authors to predict the heat transfer rate. The correlation proposed by the authors is given by

$$
Nu_{TP} = 0.56\left(\frac{U_{SG}}{U_{SL}}\right)^{0.3}\left(\mu_G/\mu_L\right)^{0.2}\mathrm{Re}_{SL}^{0.6}\,\mathrm{Pr}_L^{\frac{1}{3}}\left(\mu_B/\mu_W\right)^{0.14} \qquad (2.27)
$$

Vijay et al. (1982) developed a Reynolds analogy correlation by performing two-phase experiments in a vertical pipe by modifying Fried (1954) correlation. Incidentally, Vijay et al. (1982) correlation seems to be a good performing correlation in horizontal and near horizontal orientations based on the current experimental data. Vijay et al. (1982) correlation was modified to make the best correlation and better prediction for the current experimental data. Vijay et al. (1982) correlation is given by

$$h_{TP}/h_L = \left(\Delta p_{TPf}/\Delta p_L\right)^{0.451} \tag{2.28}$$

where

$$Nu_L = 1.615\left[\mathrm{Re}_{SL}\,\mathrm{Pr}_L\left(D/L\right)\right]^{1/3}\left(\mu_B/\mu_W\right)^{0.14} \qquad \text{(L)}$$

$$Nu_L = 0.0155\,\mathrm{Re}_{SL}^{\,0.83}\,\mathrm{Pr}_L^{\,0.5}\left(\mu_B/\mu_W\right)^{0.33} \qquad \text{(T)}$$

Bhagwat et al. (2012) performed heat transfer experiments on the current experimental setup and measured the non-isothermal pressure drop. Bhagwat et al performed experiments in vertically downward orientation and modified Vijay et al. (1982) correlation for the purpose of Reynolds analogy. The suggested correlation was able to predict all the data and performing satisfactorily with a mean error of 11.2% and standard deviation of 17.2. Bhagwat et al. (2012) correlation is also one of the best correlations in horizontal and near horizontal upward orientations for the current experimental data. The correlation suggested is

$$\frac{h_{TP}}{h_L} = \phi^{0.55} \tag{2.29}$$

where h_L is determined by Sieder and Tate (1936) equation.

Also, Oyewole (2013) performed void fraction experiments on the current experimental setup and drew flow pattern maps for the inclinations +5°, +10° and +20°. Oyewole (2013) studied the effect of flow reversal of air-mixture two phase flow in two phase inclined flows and developed models to predict the two phase flow. The author also suggested best void fraction correlation for every orientation and also for the upward inclined flow. The correlation suggested by Oyewole (2013) for upward inclination is Smith (1969) correlation which is used to calculate some of the heat transfer coefficient values which involves void fraction in them unless specified otherwise.

Table 2.1 is a comprehensive table of relevant correlations that are used to predict the current experimental data. From these correlations best performing correlations are selected and analyzed in **Table 4.1**

Table 2.1 Heat Transfer Correlations

Source	**Heat transfer Correlation**
Knott et al. (1959)	$\frac{h_{TP}}{h_L} = \left(1 + \frac{u_{SG}}{u_{SL}}\right)^{\frac{1}{3}}$ where h_L is from Sieder and Tate (1936) given by $Nu_L = 1.615\left[\mathrm{Re}_{SL}\,\mathrm{Pr}_L\left(D/L\right)\right]^{1/3}\left(\mu_B/\mu_W\right)^{0.14}$ (L) $Nu_L = 0.0155\,\mathrm{Re}_{SL}^{0.83}\,\mathrm{Pr}_L^{0.5}\left(\mu_B/\mu_W\right)^{0.33}$ (T)
Oliver and Wright (1964)	$Nu_{TP} = Nu_L\left(\frac{1.2}{R_L^{0.36}} - \frac{0.2}{R_L}\right)$ where $Nu_L = 1.615\left[\frac{\left(Q_G + Q_L\right)\rho D}{A\mu}\mathrm{Pr}_L\frac{D}{L}\right]^{\frac{1}{3}}\left(\frac{\mu_B}{\mu_W}\right)^{0.14}$

Hughmark (1965)	$Nu_{TP} = 1.75 R_L^{-0.5} \left(\frac{\dot{m}_L c_L}{R_L k_L L} \right)^{\frac{1}{3}} \left(\frac{\mu_B}{\mu_W} \right)^{0.14}$
Martin and Sims (1971)	$\frac{h_{TP}}{h_L} = 1 + 0.064 \left(\frac{u_{SG}}{u_{SL}} \right)^{0.5}$ where h_L is determined by Sieder and Tate (1936)
Aggour (1978)	$h_{TP} / h_L = (1-\alpha)^{-\frac{1}{3}}$ (L) where $Nu_L = 1.615 \left[\mathrm{Re}_{SL} \, \mathrm{Pr}_L \, (D/L) \right]^{\frac{1}{3}} \left(\frac{\mu_B}{\mu_W} \right)^{0.14}$ (L) $h_{TP} / h_L = (1-\alpha)^{-0.83}$ (T) where $Nu_L = 0.0155 \, \mathrm{Re}_{SL}^{0.83} \, \mathrm{Pr}_L^{0.5} \left(\frac{\mu_B}{\mu_W} \right)^{0.33}$ (T)
Ravipudi and Godbold (1978)	$Nu_{TP} = 0.56 \left(\frac{U_{SG}}{U_{SL}} \right)^{0.3} \left(\mu_G / \mu_L \right)^{0.2} \mathrm{Re}_{SL}^{0.6} \, \mathrm{Pr}_L^{\frac{1}{3}} \left(\mu_B / \mu_W \right)^{0.14}$
Shah (1981) for laminar	$\frac{h_{TP}}{h_L} = \left(1 + \frac{u_{SG}}{u_{SL}} \right)^{0.25}$, (for $\mathrm{Re}_{SL} < 170$) $Nu_L = 1.86 \left[\mathrm{Re}_{SL} \, \mathrm{Pr}_L \left(D / L \right) \right]^{\frac{1}{3}} \left(\mu_B / \mu_W \right)^{0.14}$
Shah (1981) for turbulent	$\frac{h_{TP}}{h_L}$ is obtained through graphical method correlation where $Nu_L = 10.023 \, \mathrm{Re}_{SL}^{0.8} \, \mathrm{Pr}_L^{0.4} \left(\mu_B / \mu_W \right)^{0.14}$
Drucker et al. (1984)	$\frac{h_{TP}}{h_L} = 1 + 2.5 \left(\alpha Gr / \mathrm{Re}_{TP}^2 \right)^{0.5}$ $Gr = \left[\left(\rho_L - \rho_g \right) g D^3 \right] / \rho_L \nu_L^2$

Kim et al. (2000)	$h_{TP} = (1-\alpha) h_L \left\{ 1 + 0.27 \left[\left(\frac{x}{1-x} \right)^{-0.04} \left(\frac{\alpha}{1-\alpha} \right)^{1.21} \left(\frac{\mathrm{Pr}_G}{\mathrm{Pr}_L} \right)^{0.66} \left(\frac{\mu_G}{\mu_L} \right)^{-0.72} \right] \right\}$
Tang and Ghajar (2007)	$h_{TP} = F_P h_L \left\{ 1 + 0.55 \left[\left(\frac{x}{1-x} \right)^{0.1} \left(\frac{1-F_P}{F_P} \right)^{0.4} \left(\frac{\mathrm{Pr}_G}{\mathrm{Pr}_L} \right)^{0.25} \left(\frac{\mu_G}{\mu_L} \right)^{0.25} \right] \left(I^* \right)^{0.25} \right\}$ $F_P = (1-\alpha) + \alpha F_S^2; \qquad F_S = \frac{2}{\pi} \tan^{-1} \left(\sqrt{\frac{\rho_G \left(V_G - V_L \right)^2}{gD \left(\rho_L - \rho_G \right)}} \right)$ $I^* = 1 + Eo \left| \sin \theta \right|; \qquad Eo = \frac{\left(\rho_L - \rho_G \right) g D^2}{\sigma}$
Reynolds Analogy Correlations	
Johnson and Abou-Sabe (1952)	$\frac{h_{TP}}{h_L} = \frac{R_L^{-0.5}}{1 + 0.006 \, \mathrm{Re}_{SG}^{0.5}} \left(\phi_L^2 \right)^{0.3333}$
King (1952)	$\frac{h_{TP}}{h_L} = \frac{R_L^{-0.52}}{1 + 0.006 \, \mathrm{Re}_{SG}^{0.5}} \left(\phi_L^2 \right)^{0.32}$ where $Nu_L = 0.023 \mathrm{Re}^{0.8} \, \mathrm{Pr}^{0.4}$
Vijay et al. (1982)	$h_{TP} / h_L = \left(\Delta p_{TPf} / \Delta p_L \right)^{0.451}$ where $Nu_L = 1.615 \left[\mathrm{Re}_{SL} \, \mathrm{Pr}_L \left(D / L \right) \right]^{1/3} \left(\mu_B / \mu_W \right)^{0.14}$ (L) $Nu_L = 0.0155 \, \mathrm{Re}_{SL}{}^{0.83} \, \mathrm{Pr}_L{}^{0.5} \left(\mu_B / \mu_W \right)^{0.33}$ (T)
Bhagwat et al. (2012)	$\frac{h_{TP}}{h_L} = \phi^{0.55}$

Having listed the general heat transfer correlations and Reynolds analogy correlations in **Table 2.1**, some of the best performing correlations are compared with the present experimental data and the performance of top performing correlations is discussed in Chapter IV. The possibility of forming best performing Reynolds analogy correlation is also noted in Chapter IV.

CHAPTER III

EXPERIMENTAL SETUP

In this chapter experimental setup and the procedure to measure the heat transfer are explained briefly. The experimental setup's key feature of variable inclination facilitated the population of data in different inclinations. The schematic of the experimental setup is shown in **Figure 3.1**.

The experimental setup was designed by Cook (2008) allowing the investigators to perform experiments involving, flow visualization, void fraction, pressure drop and heat transfer. Two different test section branches are present for different purposes. A transparent polycarbonate pipe is used for flow visualization and void fraction measurements whereas the test section branch with steel pipe and insulation is used for heat transfer. Pressure drop measurements can be carried out in either of the test branches. The current experiment focuses on the heat transfer measurements and experimental procedure. So, the experimental setup involves description of heat transfer equipment.

3.1 Description of the Experimental Setup

The current section describes the schematic of the experimental setup which is used for the measurement of non-boiling two phase air water heat transfer. The heat transfer measurements are carried in horizontal and near horizontal upward inclinations.

Flow Loop

The flow of the experimental setup is shown in the schematic **Figure 3.1**. The test platform consists of aluminum I-beam platform measuring 3.353 *m* in length and 0.61 *m* in width (11 *ft* × 2 *ft*). The flat portion is an aluminum sheet measuring 3.05 *m* × 0.61 *m*. The test sections are fastened to the platform using blocks and leather strappings. This setup is attached to variable inclination frame which moves ±90°. This can be seen in **Figure 3.2**.

Supply of Working Fluids

Air and distilled water are the working fluids used in the current experimental setup. A 55 gallon (208-litre) acts a reservoir for distilled water. A Bell & Gosset (Series 1535) coupled centrifugal pump (size 3545 D10) is used to pump the distilled water from the polyethylene reservoir. This pump draws the water from the reservoir through an Aqua-Pure AP12T water filter. An ITT standard (Model BCF 4063) one shell and two-tube heat exchanger is used to maintain the temperature of the distilled water constant by removing the constant heat added to the distilled water by the experiment. The cooling fluid used is tap water which is taken directly from the wall tap.

The distilled water flows through the Micro Motion (Model CMF125) Coriolis flow meter which is connected to a Digital Field Mount (Model RFT9739) that conditions the flow information to the data acquisition system. Control over the water flow rate is achieved by a gate valve located just after the flow meter assembly. The water then mixes with the air supply as it passes through one of the test sections and eventually returns to the 208.2 liter (55 *gal*) reservoir.

Ingersold-Rand T30 (Model 2545) air compressor serves as the air supplier. This air supply is regulated by Speedaire (Model 4ZM22) 12.7 *mm* (0.5 *in.*) regulator. The air is then cooled by passing through a copper coil submerged in a vessel of water from the wall tap. The same water from the wall tap that is used for cooling the distilled water is also used for cooling the air to ensure that both air and distilled water have the same inlet temperature. The air is then filtered by a

Speedaire (Model 4ZL49) 12.7 *mm* (0.5 *in.*) air filter to remove moisture from the air before the air flow rate is being measured. Air flow rate is regulated by a Parker Model 24NS 82(A)-V8LN-SS Needle Valve before it passes through Emerson Flow Meters (Micro MotionElite Series Model number LMF 3M and CMF025). Two flow meters are present and can be used depending on the desired working air flow range.

Air Water Mixing Section

The water and air enter the test area via a ½ *in.* IPS plastic tee. Two different mixing sections are placed in the heated section in order to help mixing. One mixer is placed at the inlet and the second one is placed at the outlet. This will lead to better accuracy to measure the temperature of the mixture. The mixers used in the setup are Koflo model 3-8 40-C-4-3V-2.

Heat Transfer Test Section

The experimental set up used for measuring two phase convective heat transfer coefficient consists of 12.5 *mm* I.D. schedule 10 S steel pipe of roughness 0.0152 *mm.* The length of the test section is 80 diameters. Large 6.35 *mm* (1/4 *in.*) thick copper plates were silver soldered at either end of the test section for use as electrical connections. The plates completely encircle the test section and are 17.8 *cm* × 17.8 *cm* (7 *in.* × 7 *in.*) in order to achieve an even distribution of current input. On the sides of the plates facing away from the heated section, 1.27 *cm* (0.5 *in.*) thick phenolic resin board has been used to help prevent loss of heat from the heated test section to the non-heated portions of the test branch.

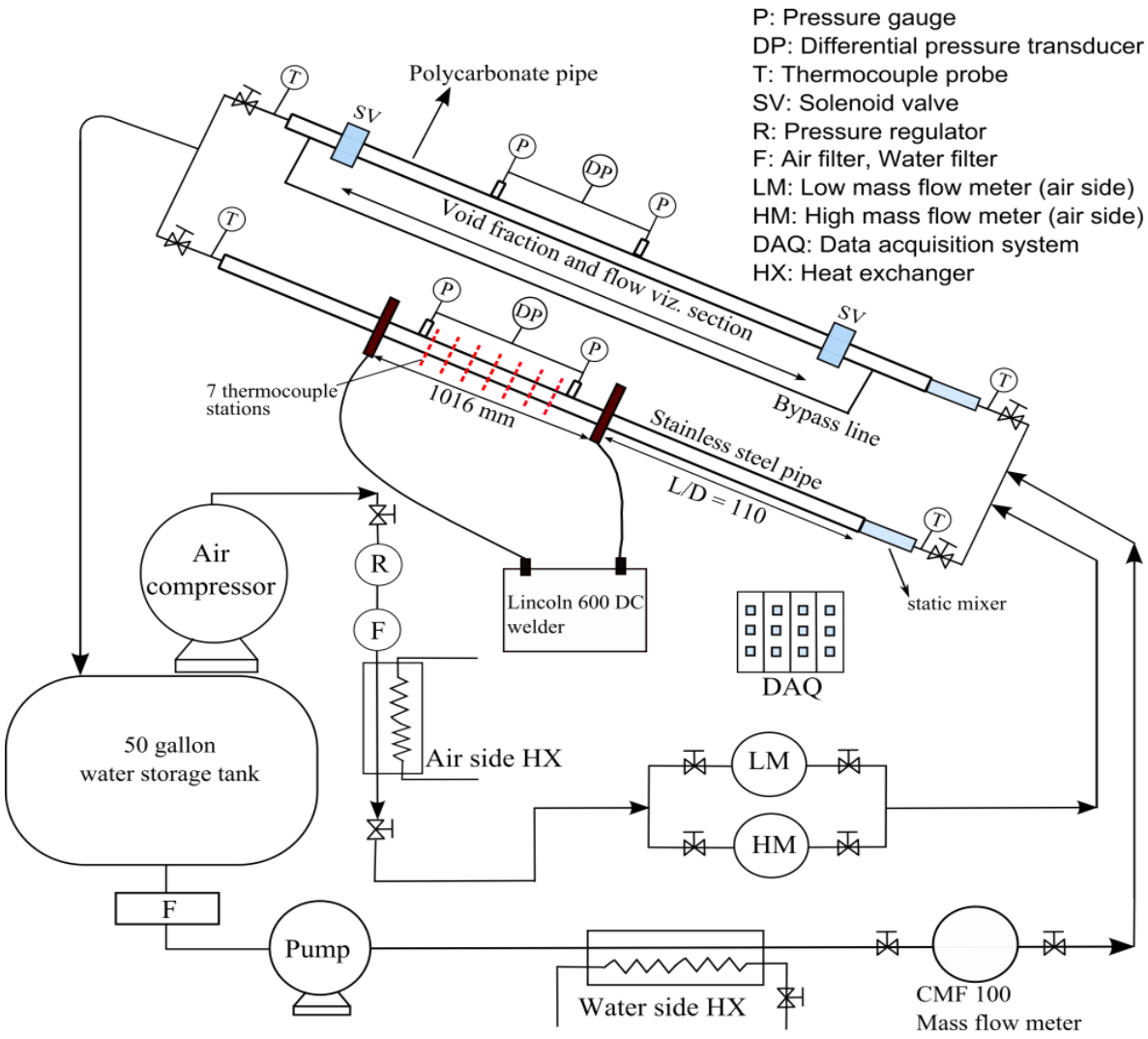

Figure 3.1 Schematic diagram of the experimental setup

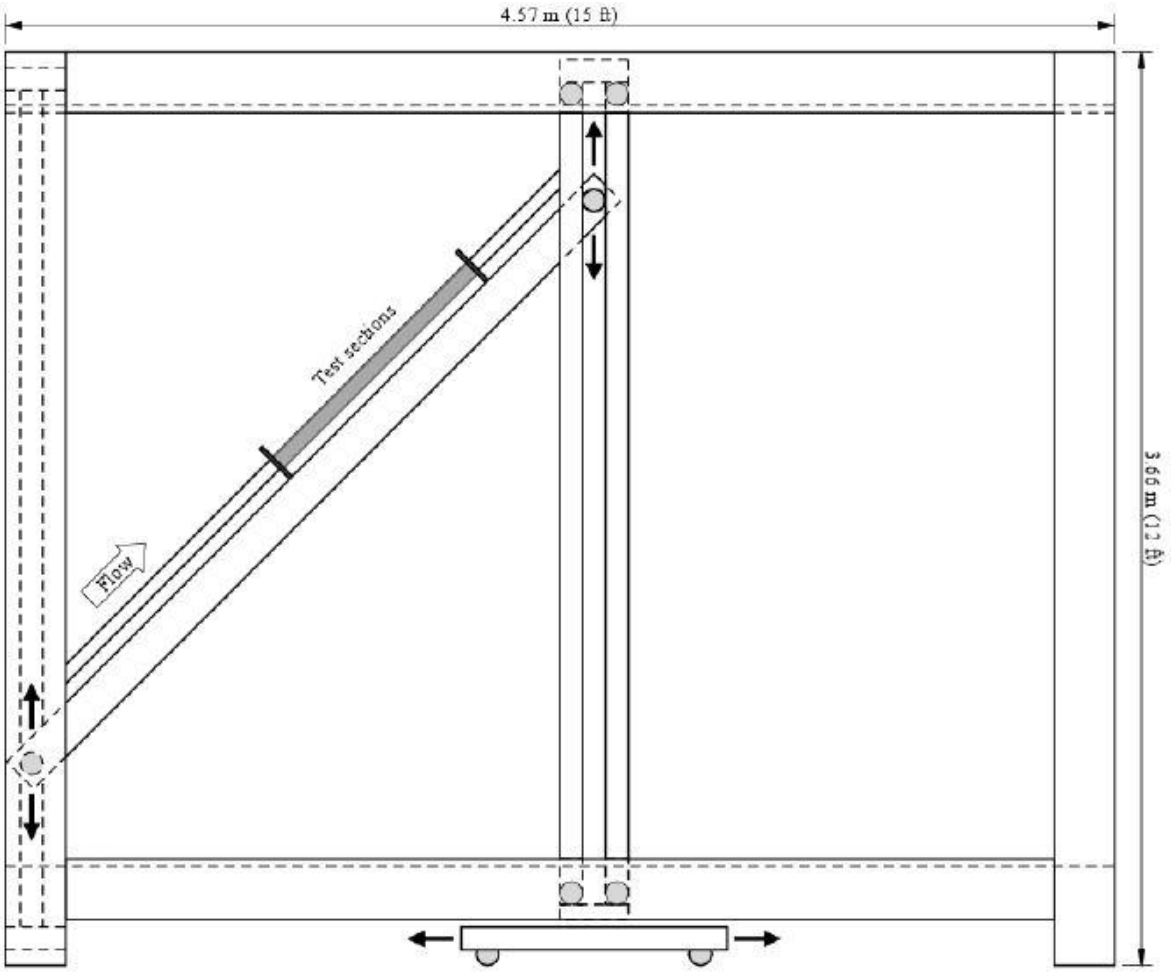

Figure 3.2 Test section with variable inclination frame

Heat Source

Current is supplied with the help of a welder. Uniform heat flux is supplied through the welder. A Lincoln Idealarc DC-600 three phase rectified electric welder, capable of producing steady output at currents of up to 750A is used to for heat transfer measurements. Connection between the plates and the welder is achieved via 4/0 AWG welding cable. On the connection plate at the exit of the heated test section, a 1000 amp shunt has been connected in line with the circuit. This shunt is manufactured by Empro Shunts and has model number B-1000-50.2.

3.2 Instrumentation

Flow Rate measurement

The water flow rate is measured by the Micro Motion (Model CMF125) Coriolis flow meter and the air flow rate is measured by the Emerson Flow Meters (Micro MotionElite Series Model number LMF 3M and CMF025). These flow meters are connected to the Digital Field Mount (Model RFT9739) which relays the flow information to the data acquisition system for data recording.

Temperature Measurements

The surface temperatures of the test section are measured with Omega TT-T-30 T-type thermocouples cemented on the test section using Omegabond 101. The mixture temperatures before and after the test section are measured with Omega TMQSS-125U-6 thermocouple probes. Thermocouples were attached in sets of four, constituting a North, South, East, West placement scheme at each point of measurement. Beginning at 12.7 *cm* (5 *in.*) from the first copper connection, seven sets of thermocouples were placed at intervals of 12.7 *cm* (5 *in.*) across the entire length of the test section. The placement of the thermocouples was symmetrical along the length of the test section. For an example of the thermocouple placement, please reference **Figure 3.3**. This type of thermocouple array allows for temperature observation around the circumference of the heated section as well as along its length.

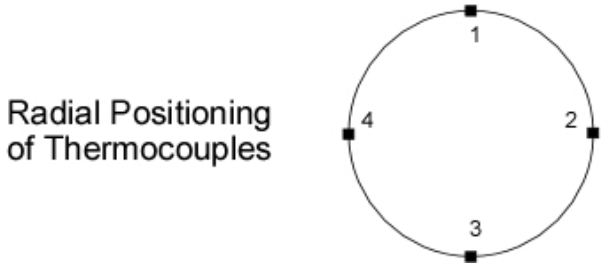

Figure 3.3 Circumferential positioning of the thermocouples

Power Measurement

The amount of input power to the experimental setup is seen from the reading obtained from the welder which is recorded by the data acquisition system. The voltage across the experimental setup is determined by the copper shunt attached to the setup. By knowing the resistance and voltage, the current across the setup can be obtained thereby giving the power input. Heat fluxes obtained by the electrical input and thermal output are obtained to check for heat balance to assure the system is working correctly.

Data Acquisition System

A National Instruments data acquisition system is used for recording and storing the data measured during the experiment. An AC powered four-slot National Instruments SCXI 1000 Chassis houses the data acquisition system. The chassis provides a low noise environment for signal conditioning. There are three National Instruments SCXI control modules housed inside the chassis: two SCXI 1102/B/C modules and one SCXI 1125 module. The graphical user interface for the data acquisition LabView Virtual Instrument was developed specifically for this experimental setup.

The LabVIEW Virtual Instrument (VI) graphical user interface provides users with the features to monitor and record data. Data such as inlet, outlet, surrounding, and test section surface temperatures, pressure drop, system pressure, air and water mass flow rates, superficial gas and liquid Reynolds numbers, and current supplied by the DC arc welder to the test section are displayed on the graphical user interface. With these features on the graphical user interface, users can monitor the recorded data and readily identify any anomaly during the course of an experiment. A former Ph.D. student Jae-Yong Kim wrote a data acquisition for a previous setup. Necessary modifications were made by another former Ph.D. student Clement Tang for the current setup.

3.3 Experimental Procedure

The experimental procedure for heat transfer has been described in detail by Cook (2008) and Tang (2011). The procedure involves in carefully initiating the experiment as it involves heat transfer of

the liquid achieved by the welders. Electricity and water is a combination which implores the investigator to ensure caution in experimenting procedure.

The initial step involves turning on instrumentation systems involving data acquisition system flow meters, LabView program and the pressure demodulator. This step also involves in checking the readings of the thermocouple readings in the stations to ensure that the LabView program for heat transfer measurements is working correctly.

The next step involves in switching on the heat exchanger for normalizing the temperature. After waiting for around 10 *min*, water pump should be switched on and the flow rate be set at near maximum. This enables the system to reach the stabilization temperature or cools down the entire setup. It has been found out through experience that efficient cooling of the setup lead to effective readings. While the pump is fully in function and the water is passing through the setup, it is advisable to check for any leaks from the tank, experimental apparatus or any of the water filters. High water flow rate will enable the investigator to notice any leaks easily.

Once, it has been made sure there are no leaks, the compressor can be switched on. The water flow rate should be decreased and the air valves can be opened to let the air inflow. By keeping the water flow rate to near minimum and increasing the air flow rate to maximum the setup should again be inspected for any leaks.

After making sure the temperature is optimum for the initiation of experimentation the welder can be switched on, initially setting at a low value and slowly increasing based on the thermocouple readings, inlet and outlet temperatures. As the desirable temperature difference is reached between the inlet and outlet the experiment can be proceeded by recording the data.

The time for recording the data depends mainly on the flow pattern. Through experience the optimum time for each flow pattern is shown below in **Table 3.1.**

Table 3.1 Estimated Time for Experimental Procedure

Flow Pattern	Recommended time	Uncertainty
Annular	7 - 10 minutes	High
Bubbly	3 – 5 minutes	Low
Wavy	5 – 6 minutes	High
Slug	3 – 5 minutes	Moderate to High

The local inside wall temperature, wall heat flux and convective heat transfer coefficient is calculated using a finite difference formulation based data reduction program developed by Ghajar and Kim (2006). The two phase convective heat transfer coefficient is represented by the average of the measured local values at each station as shown

$$h_{TP} = \frac{1}{L}\int \bar{h} dz = \frac{1}{L}\sum_{j=1}^{N_{ST}} \bar{h}_j \Delta z_j \tag{3.1}$$

3.4 Validation of Experimental Setup and Data Processing

Before starting the two-phase flow experiment after checking for all the necessary precautions, it is important to note that the setup is working correctly. So single phase heat transfer experiments are taken and compared with Ghajar and Tam (1994), Gnielinski (1976) and Sieder and Tate (1936) shown in **Table 3.2** to ensure the validity of the experimental setup. The sample calculations of uncertainty values is shown in Appendix – A.

Table 3.2 Single Phase Heat Transfer Correlations

Author	Correlation
Sieder and Tate (1936)	$Nu_L = 1.615\left[\mathrm{Re}_{SL}\,\mathrm{Pr}_L\left(D/L\right)\right]^{1/3}\left(\mu_B/\mu_W\right)^{0.14}$ (L) $Nu_L = 0.0155\,\mathrm{Re}_{SL}^{0.83}\,\mathrm{Pr}_L^{0.5}\left(\mu_B/\mu_W\right)^{0.33}$ (T)
Gneilinski (1976)	$Nu_L = \dfrac{\left(\frac{f}{8}\right)(\mathrm{Re}-1000)\,\mathrm{Pr}}{1+12.7\left(\frac{f}{8}\right)^{0.5}\left(\mathrm{Pr}^{\frac{2}{3}}-1\right)}$ where, $f = \left(0.79\ln(\mathrm{Re})-1.64\right)^{-2}$
Ghajar and Tam (1994)	$Nu_L = 0.023\mathrm{Re}^{0.8}\,\mathrm{Pr}^{0.385}\left(L/D\right)^{-0.0054}\left(\mu_B/\mu_W\right)^{0.14}$

Single Phase Flow Uncertainty

The uncertainty of the populated single phase heat transfer experimental data is calculated using Kline and McClintock (1953) uncertainty analysis. This is clearly shown in Appendix A. A total of 19 data points collected with Re_L ranging from 1300 to 26,000. The maximum and minimum uncertainties for the data was found to be ±12.08% and ±5.31%, respectively. It is observed that the uncertainty values for low liquid flow rates is more than that of high liquid flow rates which also reflects in two phase heat transfer uncertainty. The uncertainty compared with the single phase heat transfer correlations is shown in **Figure 3.4**. The average and standard deviation of single phase heat transfer coefficient with respect to the Gnielenski (1976) correlation is 4.8% and 14.82% and for Ghajar and Tam (1994) is 0.86% and 3.7%.

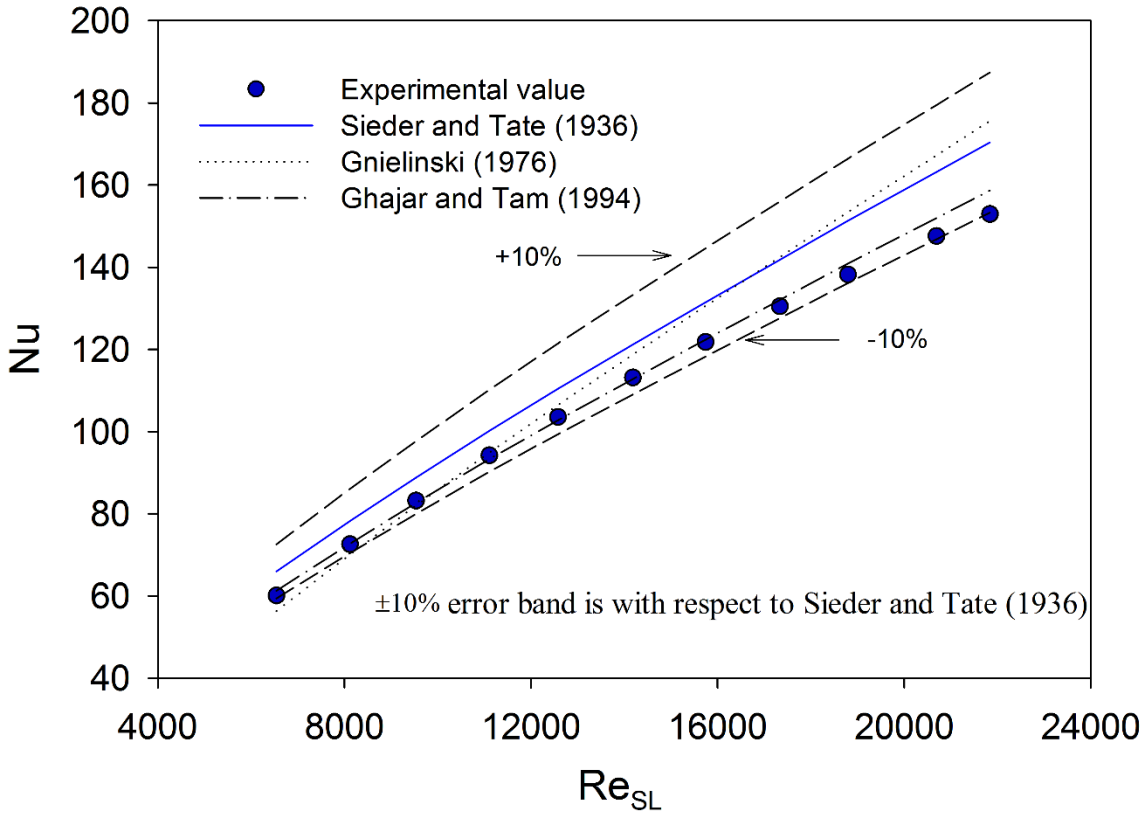

Figure 3.4 Uncertainty of single phase Nusselt number

Two Phase Flow Uncertainty

High uncertainty in the measured heat transfer coefficient is found in the annular flow region. This is expected as the heat transfer in annular flow region becomes difficult to measure due to a small temperature difference between inlet and outlet. It is also to be noted that for bubbly and slug flows, the uncertainty values are considerably lower. For the flows which are affected by both gravity and inertia in upward inclination, like wavy flows, the uncertainty varies to a greater extent. In intermittent flows, including slug wavy or wavy annular flows, the flow boundaries are hugely affected by the change in orientation and gravitation. Heat balance error also seems to affect the

uncertainty. In slug flows the heat balance error tends to be at maximum of 3.40% while in annular flows the heat balance error is found to be up to 12% for higher pipe orientations. The heat balance error for intermittent flows is in a range of 5.65% to 10% for the low, moderate or high mass flow rates of water. **Table 3.3** summarizes the minimum and maximum uncertainty in the measured two phase heat transfer coefficient for different flow patterns and pipe orientations.

Table 3.3 Minimum and Maximum Uncertainties in Different Flow Patterns and Pipe Orientations

Flow Pattern		**5°**	**10°**	**20°**	**0°**
Stratified	Min %	-	-	-	27
	Max %	-	-	-	10
Intermittent	Min %	13.56	12.03	13.13	25
	Max %	30.26	28.12	25.85	11
Slug	Min %	12.04	12.27	12.30	13
	Max %	16.87	15.97	16.47	9
Bubbly	Min %	11.66	10.89	10.86	12
	Max %	11.06	11.64	11.79	10
Wavy	Min %	14.72	15.40	15.08	-
	Max %	23.20	22.01	21.42	-
Annular	Min %	15.57	16.86	15.85	-
	Max %	34.92	32.76	29.58	-

CHAPTER IV

RESULTS AND DISCUSSION

The study of the effect of pipe orientation on two phase flow is important since it is found that the variations in most of the two phase flow parameters for constant gas and liquid flow rates are related to the flow patterns which in turn are directly affected by the change in pipe orientation. The different two phase flow patterns are generated due to the compressibility nature of the gas phase and significantly different physical properties of the two phases. A careful mapping of the flow patterns is essential for the estimation of the sequence of appearance of different flow patterns with change in the gas and liquid flow rates. It should be noted that the definitions of flow patterns and their transitions are highly qualitative in nature and are mostly based on the individual's perception of the physical structure of two phase flow patterns. Other methods such as power spectral analysis of the pressure drop signal and probabilistic flow regime mapping are introduced recently in the two phase flow literature however; these methods are very much specific to the flow conditions and are indirectly based on some reference to the visual flow pattern observation. In the present study, the key flow patterns observed in horizontal and upward inclined two phase flow are bubbly, slug, intermittent, stratified and annular flow regimes. These flow patterns are generated by varying the gas and liquid flow rates (superficial gas and liquid Reynolds numbers) in a range of 0.003 *kg/min* to 0.2 *kg/min* (Re_{SG} = 200 to 20,000) and 1.5 *kg/min* to 12.5 *kg/min* (Re_{SL} = 2000 to 18,000), respectively. The superficial gas and liquid Reynolds number is defined in terms of superficial

phase velocity, phase density and viscosity and pipe diameter as represented in Eqs. (4.1) and (4.2) The flow visualization is carried out in transparent polycarbonate pipe using Nikon D3100 camera and 200mm f/5.6 lens with a shutter speed of 1/4000 s.

$$\mathrm{Re}_{SG} = \frac{\rho_G D U_{SG}}{\mu_G} = \frac{GxD}{\mu_G} \tag{4.1}$$

$$\mathrm{Re}_{SL} = \frac{\rho_L D U_{SL}}{\mu_L} = \frac{G(1-x)D}{\mu_L} \tag{4.2}$$

4.1 Flow Patterns and Flow Pattern Maps

In horizontal flow, four distinct patterns have been observed namely bubbly, slug, annular and wavy by Ghajar and Bhagwat (2014). In the upward inclination specifically four distinct flow patterns namely bubbly, slug, wavy and annular have been observed by Oyewole (2013). The current experiment follows the similar flow rates of that of Oyewole which were collected on the same experimental setup. The intermittent flow regimes categorized by the transitioning and chaotic nature of the flow pattern have been observed and classified such as, slug-wavy, wavy-annular and slug-bubbly.

Bubbly Flow

The bubbly flow regime is characterized by the dispersion of small gas phase bubbles in the continuous liquid medium near the pipe top wall. Two kinds of bubbly flow was observed by Oyewole (2013). Bubbly flow has been observed at high liquid flow rates with low and moderate gas flow rates. Dispersion of the bubbles takes place with the increase of liquid flow rates shearing the bigger bubbles to smaller and dispersed ones. The bubbles are observed at the top surface of the plate in horizontal and near horizontal flows due to the buoyancy effects observed in upward inclined flows.

Slug Flow

The slug flow is identified as a flow structure consisting of elongated gas slugs of varying lengths and frequency that flow alternate to a liquid plug. In horizontal flows, slug lengths vary with the variation of the gas and liquid flow rates. Oyewole observed slug flow for very low liquid and low gas flow rates till moderate gas flow rates in inclined flows. Varied lengths and frequencies of slug are due to the conflicting effects of gravitational and buoyancy in upward direction.

Wavy Flow

Wavy flow is observed by Oyewole (2013) for moderate to high gas flows and moderate to high liquid flow rates. Wavy flow is explained by the with Kelvin-Helmholtz instability theory which shows the transition to turbulent flow. Typically for Re_{SG} = 7000 to 9000 and Re_{SL} = 7000 to 10000. In horizontal orientation the waves are known to wet the top surface of the pipe. But due to the gravitational forces, this is not possible in inclined flows.

Annular Flow

The annular flow is observed in form of liquid film flowing in contact with the pipe wall that surrounds a fast moving gas core. Theoretically, the annular flow is defined as a flow of two phases flowing separately. However, in practice, the annular flow is accompanied by significant entrainment of the liquid droplets into the fast moving gas core. This entrainment is quite noticeable for high liquid flow rates and gradually reduces with decrease in the liquid flow rates. It's expected that the two phase annular flow with liquid entrainment will increase the two phase heat transfer due to added turbulence in comparison to the quasi equilibrium (no entrainment) annular two phase flow that may occur for very low liquid flow rates.

Stratified Flow

The stratified flow is featured by the gas phase flowing parallel to the liquid phase at the bottom wall of the pipe. Stratified flow is completely absent in upward inclination. The flow usually skips stratification and turns to wavy as the liquid and gas phase change from very low flow rates to moderately low flow rates.

Intermittent Flow

In the present study, the intermittent flow pattern is identified based on the pulsating, chaotic and wavy nature of the two phase flow that lacks a specific alignment of the gas phase with respect to the liquid phase. Thus the flow structure tagged as intermittent flow in the present study comprises of slug-wavy, stratified-wavy and annular-wavy flow patterns for moderate liquid and moderate gas flow rates, low liquid and moderate gas flow rates and low to moderate liquid and high gas flow rates, respectively.

The slug wavy flow is marked by vigorously moving distorted slug and is characterized by the entrainment of tiny bubbles in both elongated gas bubble and the liquid slug. The slug wavy flow may be referred to as a chaotic version of slug flow that helps to enhance two phase heat transfer. The definition of stratified wavy flow that appears only in horizontal pipe orientation is the wavy and unstable gas liquid interface. In this subcategory of intermittent flow, the increase in liquid and gas flow rates caused the gas-liquid interface to become wavy with momentarily touching (splashing) of the liquid phase to the pipe top wall. In wavy annular flow, the liquid film thickness at pipe bottom wall is considerable compared to that at the pipe top wall. The liquid film at the pipe top wall is supported mostly due to the continuous splashing of the liquid however, sometimes a few dry spots are also observed. The observed flow patterns can be shown as a representation in **Figure 4.1**.

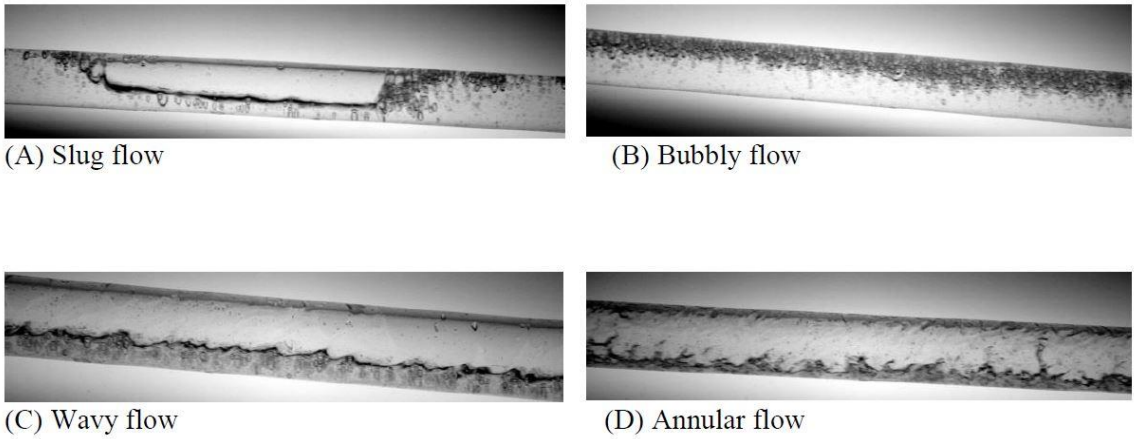

Figure 4.1 Flow patterns observed by Oyewole (2013)

In the current experiment, the horizontal flow map is plotted by Ghajar and Bhagwat (2014 a).This flow map is shown in **Figure 4.2**. All the upward inclined data is compared with respect to the horizontal data to understand the increase or decrease of heat transfer coefficient. For this purpose, it would be advantageous to combine the flow patterns of different orientations for better understanding of the effect of inclination on the flow pattern map.

Also, this flow pattern map is modified and upward inclinations are accommodated by Ghajar and Bhagwat (2014 b). This gives a total picture on the flow maps and the flow study involved in this experiment. The **Figure 4.3** gives the comprehensive picture of the all the inclinations in the present study.

This effect of inclination on the flow pattern has been discussed by Oyewole (2013) in detail making flow pattern maps. The void fraction data collected and analyzed by Oyewole (2013) recommends the best void fraction correlation for upward inclined flow.

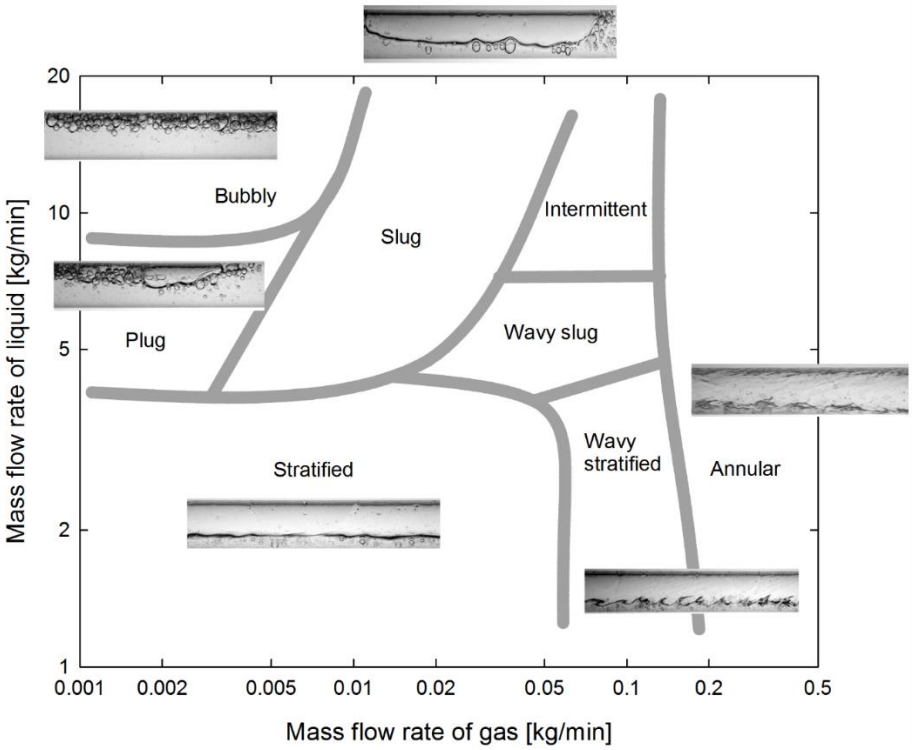

Figure 4.2 Flow patterns for horizontal orientation by Ghajar and Bhagwat (2014 a)

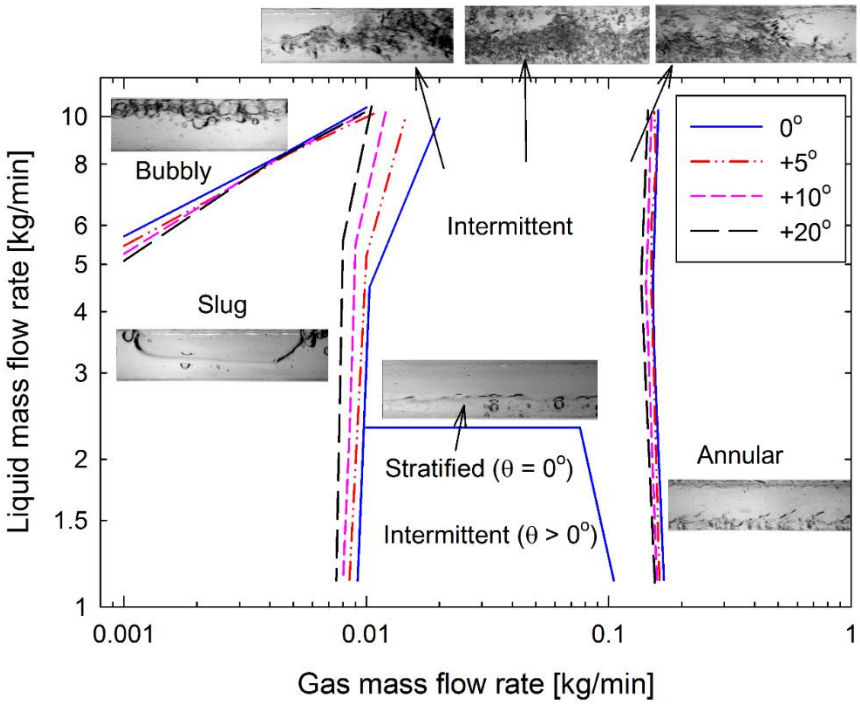

Figure 4.3 Flow regime map for horizontal and upward inclined two phase flow by Ghajar and Bhagwat (2014 b).

For horizontal pipe orientation, at low liquid flow rates, increase in the gas flow rate causes the flow pattern to shift from stratified to intermittent and finally to annular flow. The intermittent flow between stratified and annular flow may be classified as wavy annular flow having physical structure described above. Whereas, for moderate liquid flow rates, the flow pattern transits from slug to intermittent to annular flow as the gas flow rate is increased from low to moderate to high flow rates. It is also evident from this flow pattern map that the transition boundaries between different flow patterns with the exception of boundary between intermittent and annular flow are influenced by the change in pipe orientation. It should be noticed that for horizontal flow, there is no stratified flow pattern for gas mass flow rates lower than 0.01 kg/min and in upward inclined pipe orientations stratified flow is completely absent.

Most of the data points collected in the current experiment are in intermittent region. It is important to note that the definition of intermittent flow patterns usually depends on the observer performing the flow visualization. Though there might be a change in the definition, flow physics remains the same for the given gas-liquid flow rate at that particular condition.

4.2 Flow Reversal

A peculiar phenomenon observed in upward inclined two phase flow is the 'flow reversal'. Flow reversal in upward pipe inclinations results from the interaction of buoyancy, inertia and gravity forces and is a consequence of dominant gravity force acting on the liquid phase that tends to pull the liquid phase back while the gas phase moves in the upward direction. In the present study, flow reversal is observed for low values of liquid and gas flow rates typically $Re_{SL} < 5000$ and $Re_{SG} < 2000$. The flow reversal is observed by visual observation when the liquid layer near the pipe wall (bottom) is found to move in the direction opposite (downward) to that of the mean flow (upward). Based on the flow visualization it is found that the flow reversal phenomenon depends on the pipe orientation to a considerable extent and the range of gas flow rates over which the flow reversal is directly proportional to the pipe orientation. The two phase flow literature reports experimental

work related to flow reversal for vertical upward flow with hardly any information available for upward inclined systems. Typically, two phase flow literature acknowledges the existence of flow reversal by finding the frictional pressure drop minimum after which the frictional pressure drop increases consistently with increase in the gas flow rates indicating end of flow reversal regime.

Flow reversal in two phase flow was observed by Taitel and Dukler (1976) in vertically upward flows. It was described to be as the inverse of flooding and observed when the gas flow rate is changed from high flow rate to low flow rate leading to a partial down flow of the liquid. This counter-current flow leads to the shearing of the liquid film by the gas in the direction opposite to the mean flow of the liquid. This phenomenon is studied by Oyewole (2013) and a dynamic pressure model is developed to predict the flow reversal of two-phase flow in near horizontal upward inclined pipes.

Flow reversal phenomenon complicates the heat transfer analysis due to its nature. No definite conclusions can be drawn from the heat transfer analysis during the occurrence of flow reversal phenomenon. Heat transfer analysis becomes problematic and unreliable due to the presence of dry spots as a consequence of low liquid and low gas flow rates while supplying constant heat flux. Though secondary flows are quite common in affecting the heat transfer, heat transfer analysis in flow reversal region - very low liquid and gas flow rates should be avoided.

4.3 Heat Transfer in Horizontal and Near Horizontal Orientations

Considering the dependence of flow structure on the pipe orientation, this experimental study attempts to study the combined effect of the flow pattern and change in pipe orientation on two phase heat transfer coefficient. This combined effect is studied by varying the inclination of the pipe in the upward direction with measurements carried out at similar gas and liquid mass flow rates at all orientations.

Figure 4.4 shows the variation of two phase heat transfer coefficient measured for varying gas and liquid flow rates. The liquid flow rate ranged from 1.5 to 5 kg/min ($2000 < Re_{SL} < 12,500$) and the gas flow rate ranged from 0.003 to 0.2 kg/min ($200 < Re_{SG} < 20,000$). The flow pattern corresponding to each combination of Re_{SG} and Re_{SL} is also identified for better understanding of the flow pattern effect on h_{TP}.

For $1000 < Re_{SG} < 10,000$ and $Re_{SL} = 2600$ stratified flow is observed in the horizontal orientation which is shear driven in nature. As the flow is co-current, no resistance is offered to the inertial force of the liquid. The gas layer moves on top of the wavy and unstable liquid layer creating a disturbance wave that increases the heat transfer rate. For $Re_{SG} < 1000$ and $Re_{SL} < 12,100$ slug flow is observed in horizontal and upward inclined systems. Bhagwat et al. (2012) and Oliver and Wright (1964) observed that the two phase heat transfer coefficient in slug flow regime is a function of slug length and slug frequency. The magnitude of h_{TP} is observed to increase with increasing slug frequency that corresponds to short length slugs and decreases with decrease in slug frequency associated with large length slugs. This relation between h_{TP} and slug length and slug frequency is anticipated since fast moving slugs would result into lower residence time of the gas phase in the test section (smaller contact time of the gas phase with the pipe wall) and hence increase in the heat transfer coefficient. The opposite must hold true for slow moving long slugs.

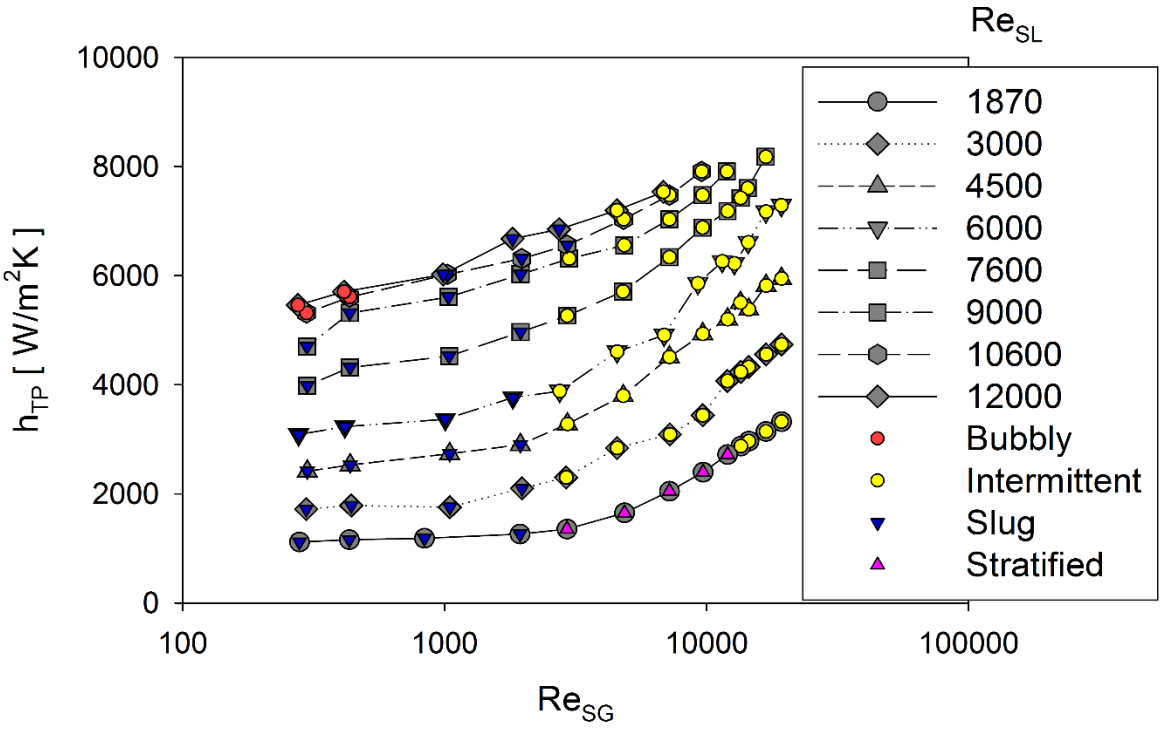
Re_SL
1870
3000
4500
6000
7600
9000
10600
12000
Bubbly
Intermittent
Slug
Stratified
h_TP [W/m^2K]
Re_SG
10000
8000
6000
4000
2000
0
100
1000
10000
100000

(a) 0°

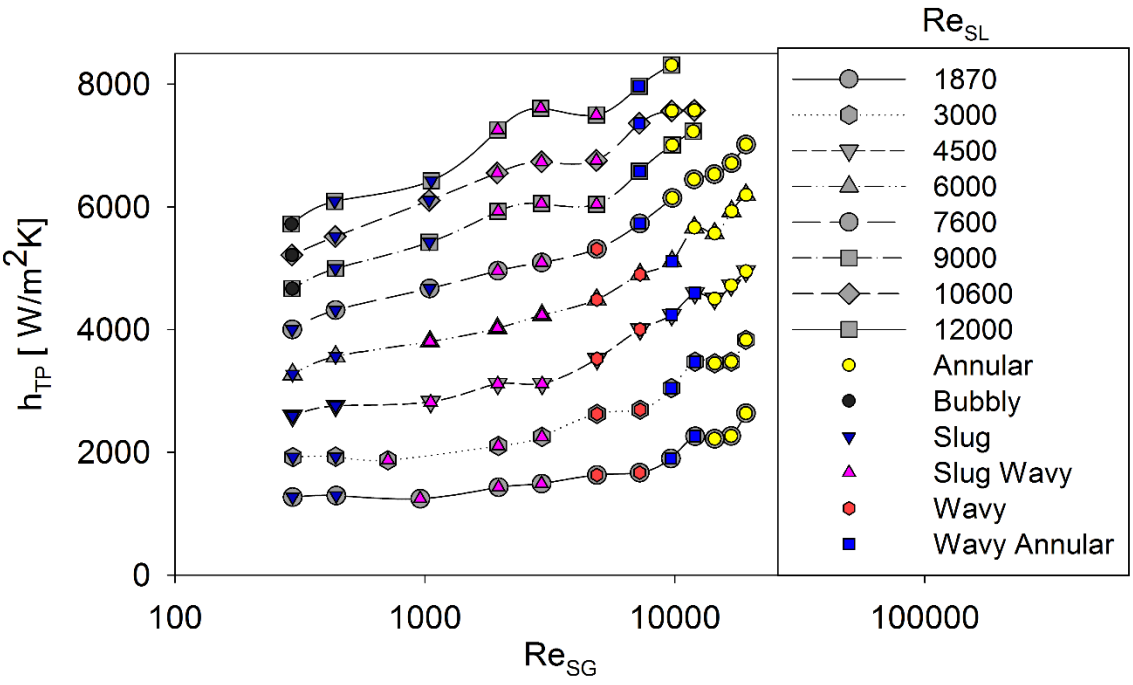
Re_SL
1870
3000
4500
6000
7600
9000
10600
12000
Annular
Bubbly
Slug
Slug Wavy
Wavy
Wavy Annular
h_TP [W/m^2K]
Re_SG
8000
6000
4000
2000
0
100
1000
10000
100000

(b) + 5°

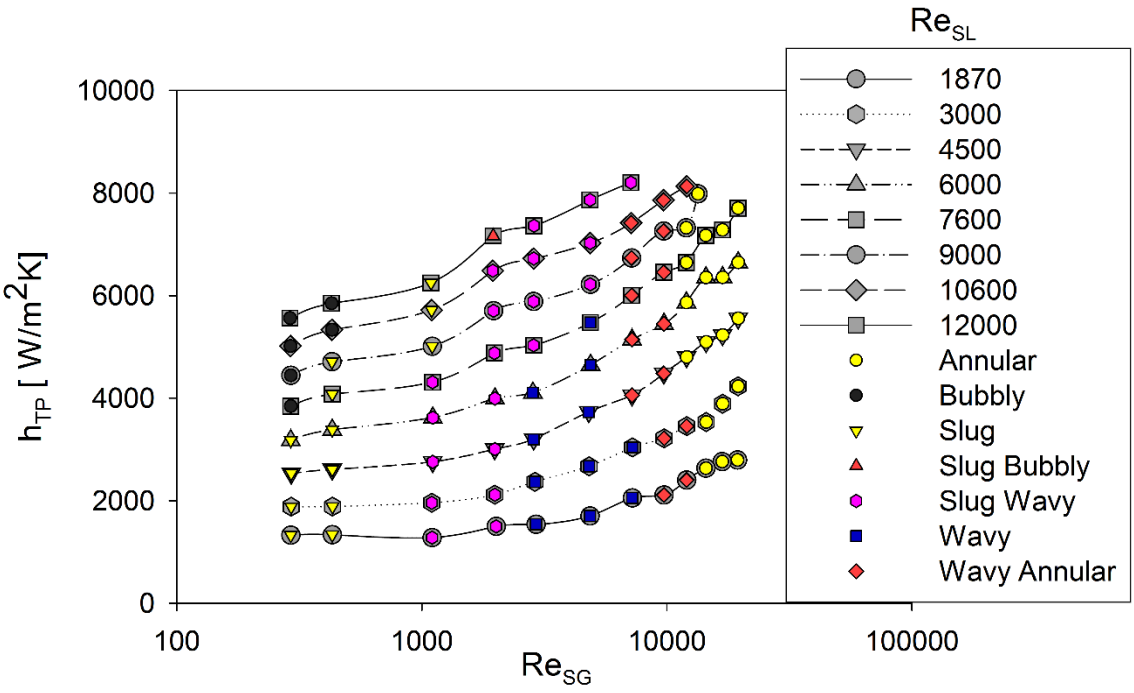

(c) + 10°

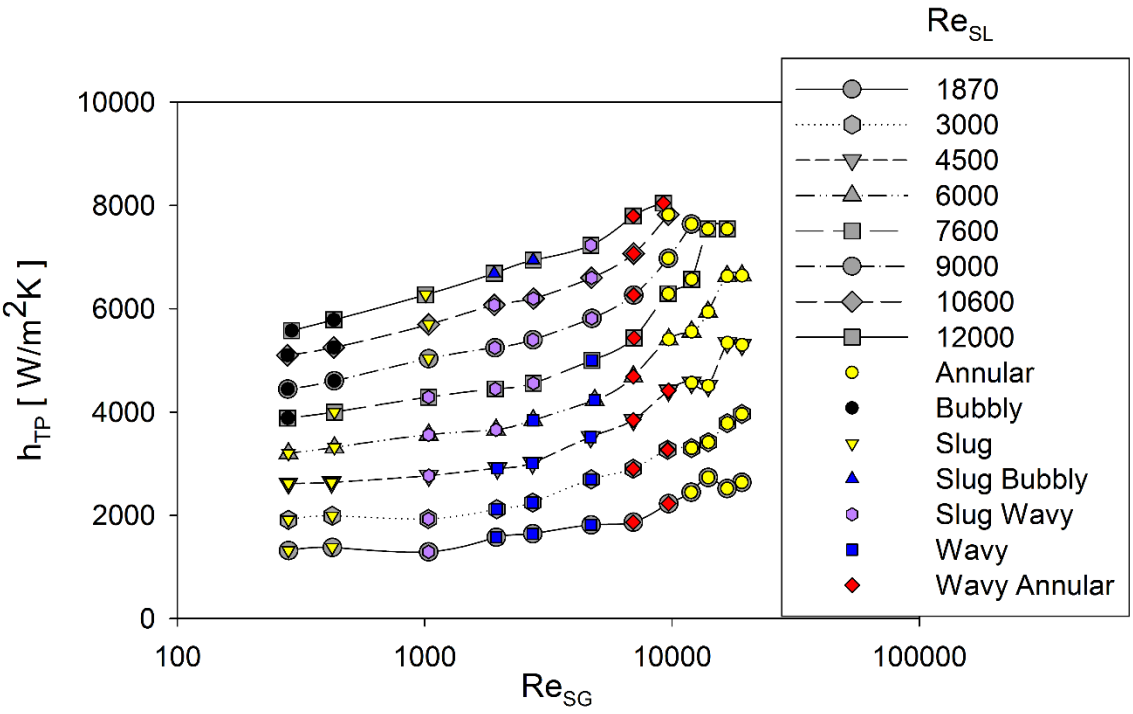

(d) + 20°

Figure 4.4 Variation of two phase heat transfer coefficient at fixed Re_{SL} and increasing Re_{SG}

(a) 0 degree, (b) +5 degree, (c) +10 degree, (d) +20 degree.

As disused so far, it is evident that the heat transfer in upward inclination is heavily dependent on the physical structure of flow pattern and also the pipe inclination. For a slug-wavy flow we see maximum heat transfer in +5° as a result of wetting of the top surface. This phenomenon also occurs for +10° flow in wavy region. For +20° flow, the waves cannot wet the top surface as pipe orientation and gravitational forces act to suppress the wave rise. In the slug flow regime Tang (2011) observed that as the inclination is increased to an angle greater than +5°, the slug collapsed on itself without any apparent increase in the heat transfer. Also, slight decrease in heat transfer coefficient was observed when this phenomenon takes place. In the current experiment, this phenomenon is observed even in the slug wavy region. For Re_{SL} = 7600 and varying Re_{SG} from 2000 to 12000, this can be illustrated by examining the peripheral heat transfer coefficient for different flow patterns in the pipe.

As the top surface of the pipe is repeatedly wetted by the waves in slug-wavy region, it should also follow that the heat transfer in slug wavy region on the top surface of the pipe in +5° should be greater than that of +10° and +20°**.** It should also be noted that the bottom surface heat transfer coefficient is greater than that of top surface in slug flow regime which is in consistent with the observations made by Shoham et al. (1982). In wavy region it is observed that h_{TP} of the top surface in +10° is very close to that of +5° establishing the advent of wetting of top surface at +10°. In wavy annular region, the peripheral heat transfer coefficient at every radial position in +10° is greater than the other two inclinations. In annular region the peripheral heat transfer coefficient in all the three inclinations are very close to each other. This is illustrated in **Figure 4.5.** This is also reflected in the percentage of increase with respect to horizontal which can be seen in **Figure 4.6.**

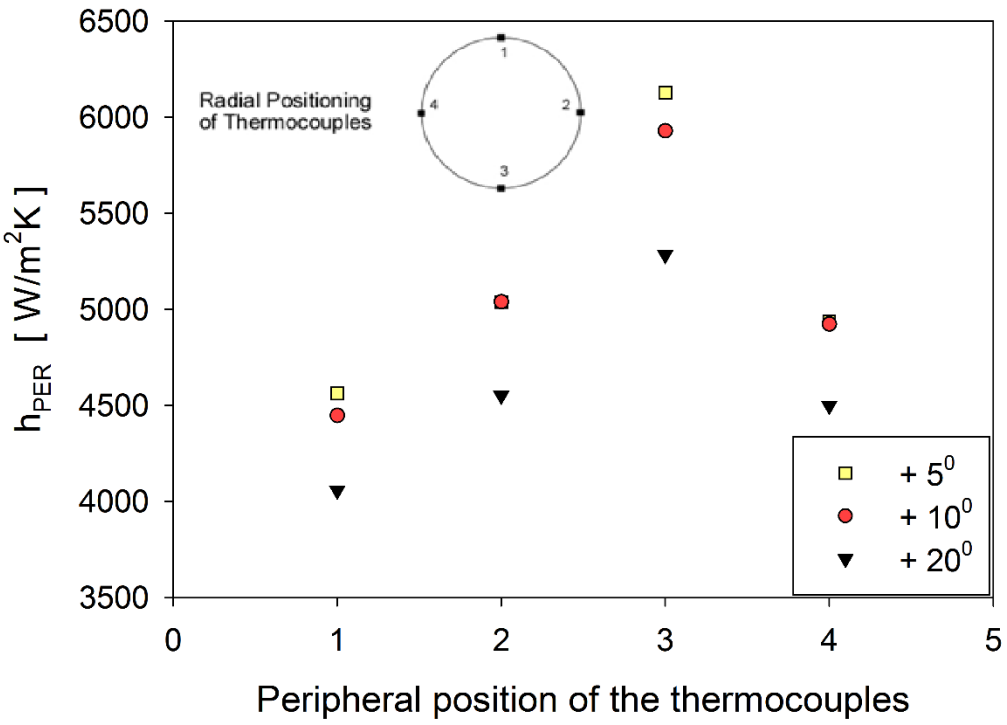

(a) Slug-Wavy

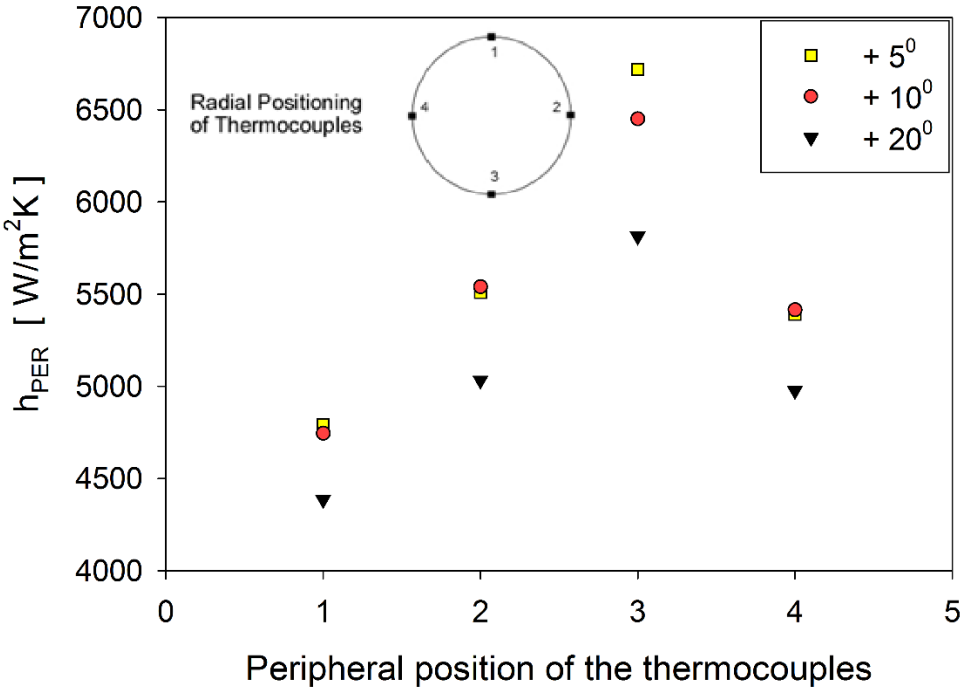

(b) Wavy

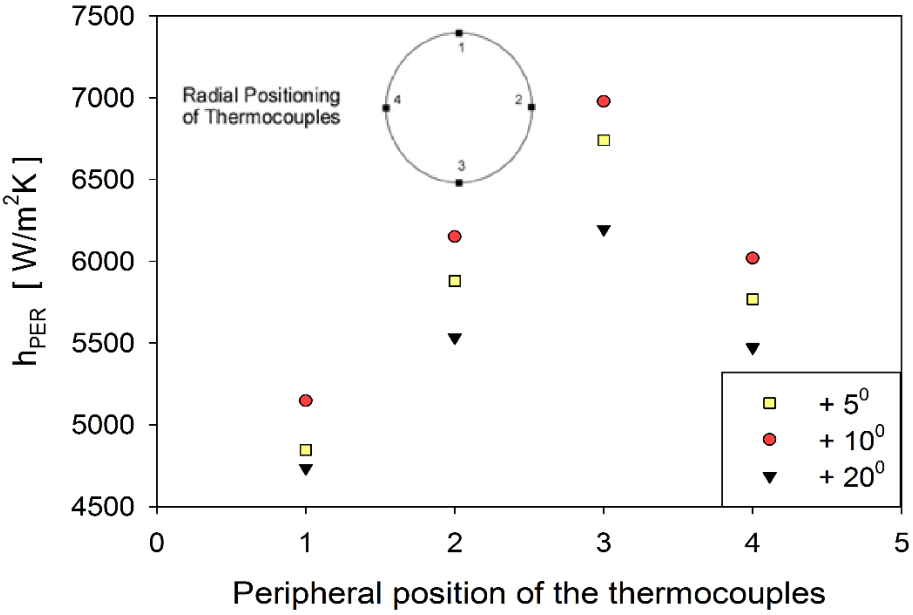

(c) Wavy Annular

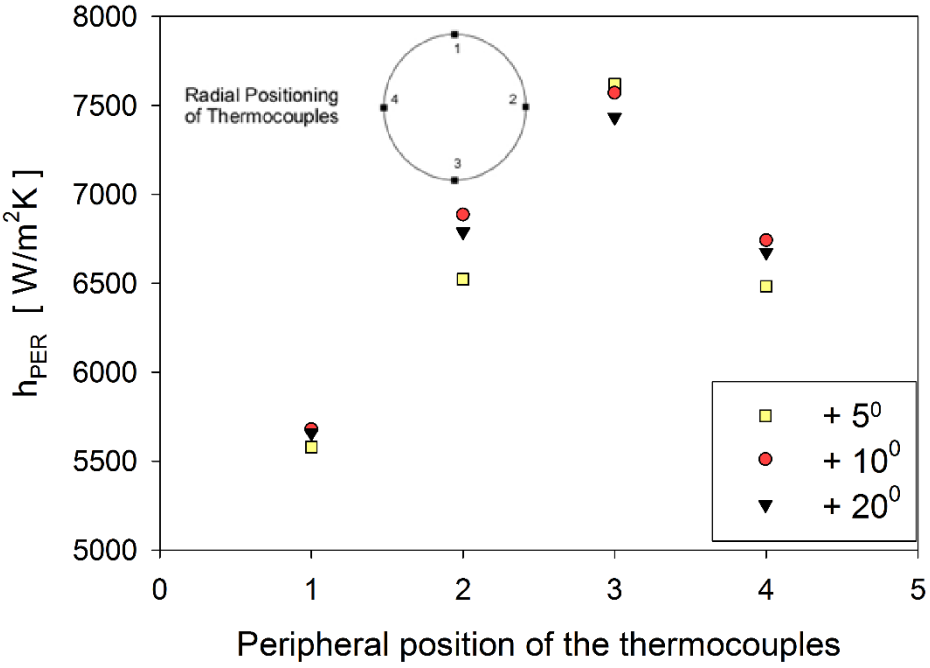

(d) Annular

Figure 4.5 Peripheral heat transfer coefficient in different flow patterns

The comparison percentage increase in the heat transfer between different orientations with reference to horizontal flow is shown in **Figure 4.6.** It would also be interesting to know the level of enhancement in terms of numbers to get a clear understanding of the effect of the pipe orientation on h_{TP}. For slug/slug wavy flow regime the maximum increase of 15% was observed in +5° pipe orientation. As the flow pattern is changed to wavy and annular regime a consistent increase in h_{TP} of about 10% in +10° is observed whereas for +20° it was between 0.5% and 5%. For low values of gas flow rates ($Re_{SG} < 5000$), the lower values of h_{TP} and large percentage change in h_{TP} are essentially due to the existence of flow reversal in upward inclined systems. It is also observed that as the flow pattern changes from wavy to wavy annular/annular, the increase of heat transfer in $+5^o$ and $+20^o$ (about 5%) which is not as much as it is in $+10^o$ (10%) accounting for the maximization of heat transfer in +10° for most of the populated data.

In **Figure 4.7** we observe that for slug flows the effect of pipe orientation on two phase heat transfer coefficient is negligible at low gas flow rates (flow reversal region), but for $Re_{SG} > 4500$, the effect of pipe orientation on h_{TP} is noticeable for different flow patterns. At +20° pipe orientation, a steep increase of h_{TP} is observed at $Re_{SG} = 17{,}000$ after the flow transits to wavy annular. This increase in h_{TP} is probably because unlike in wavy region, a thin liquid film is always in contact with the pipe upper wall that aids two phase heat transfer in wavy annular flow. A slight increase in h_{TP} is observed further this point for low values of Re_{SL}. This average increase in h_{TP} observed in the present study for $Re_{SL} = 4500$ is about 6%. At higher liquid flow rates ($Re_{SL} > 10{,}000$) we observe the effect of slug-wavy flow on h_{TP} in the inclined orientations. For +5° it dramatically increases the h_{TP} and falls as the flow changes from slug wavy to wavy annular. Also, as the Re_{SL} increases gradually, the difference between h_{TP} at inclined pipe orientations and horizontal is gradually increased which is clearly illustrated in **Figure 4.7**. For high values of gas flow rates ($Re_{SG} > 5000$), waves are developed on the liquid surface and there is not a significant difference in the flow structure. However, a minute observation of the wavy liquid surface reveals that in case of horizontal flow 'rolling waves' are observed that are in contact with the pipe upper wall quite often

in comparison to the 'wave undercutting' observed in upward inclined flows. In wave undercutting process the wavy liquid surface is tore off by the fast moving gas and the torn liquid ligament moves in a direction opposite to that of the mean flow. However, in case of 'rolling wave' process, the gas phase rolls the liquid crests in the downstream direction possibly without detaching it from the liquid surface. This perhaps promotes a local acceleration of the liquid phase that enhances two phase heat transfer coefficient in horizontal orientation. In upward inclination the 'wave undercutting' affects the orientations above +10° reducing the two phase heat transfer coefficient.

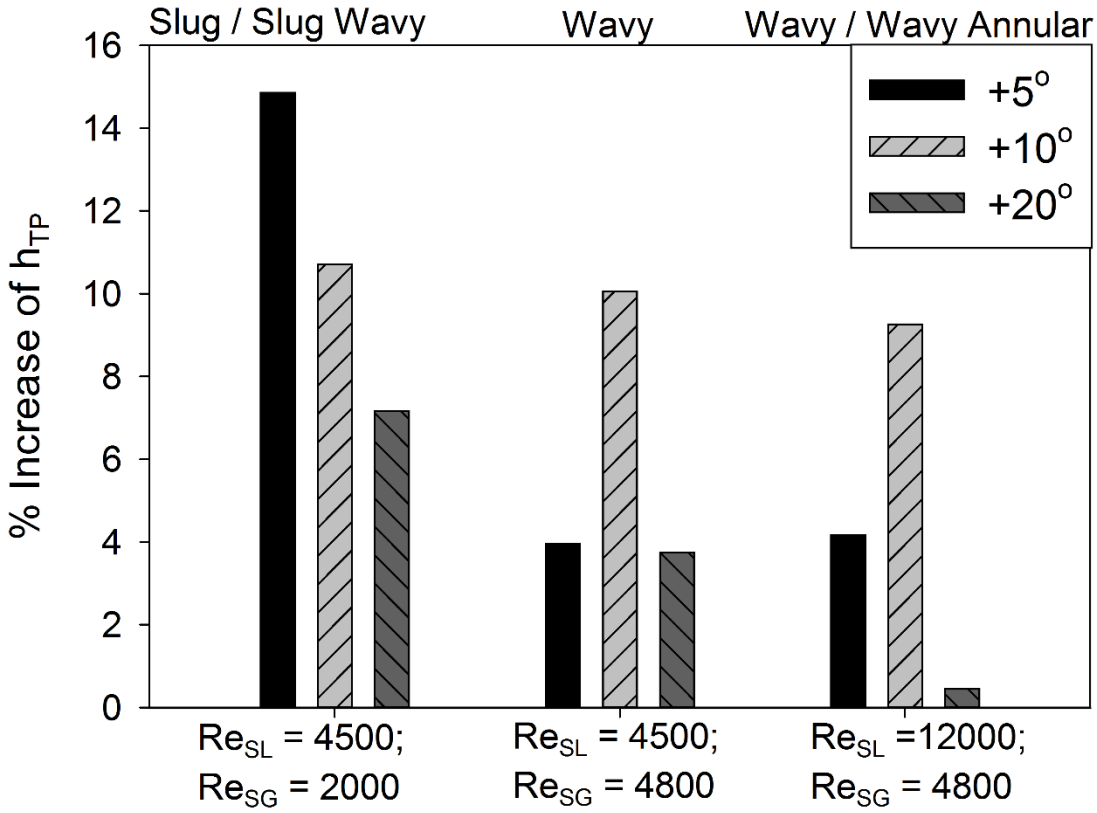

Figure 4.6 Percentage change in h_{TP} for different inclinations with reference to horizontal orientation.

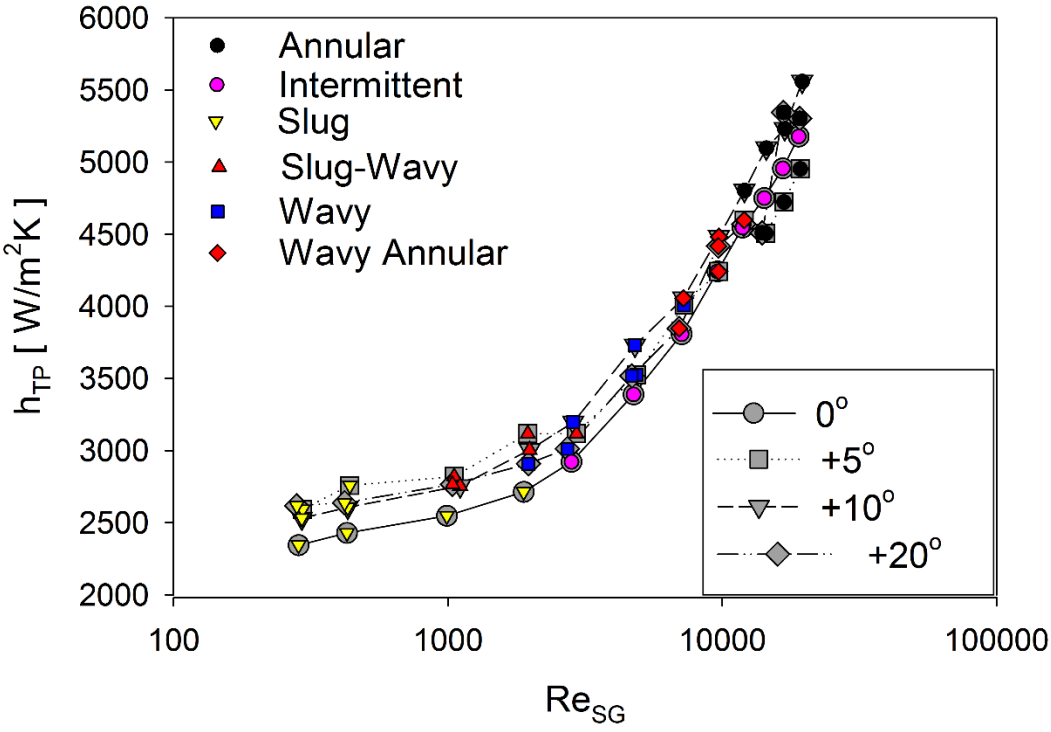

(a) Re_{SL} = 4500

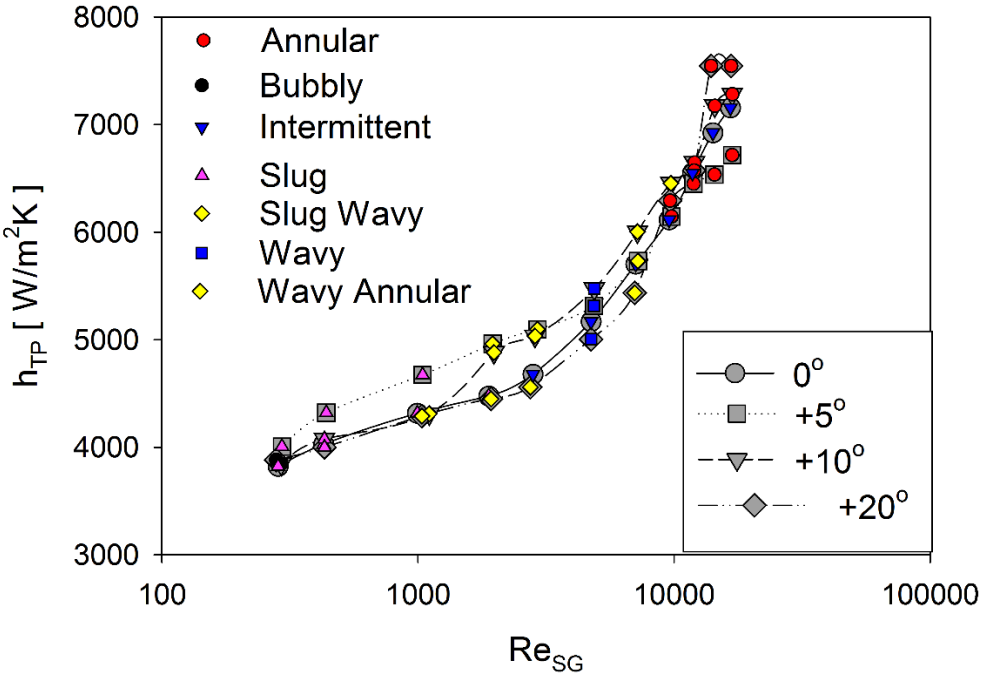

(b) Re_{SL} = 7600

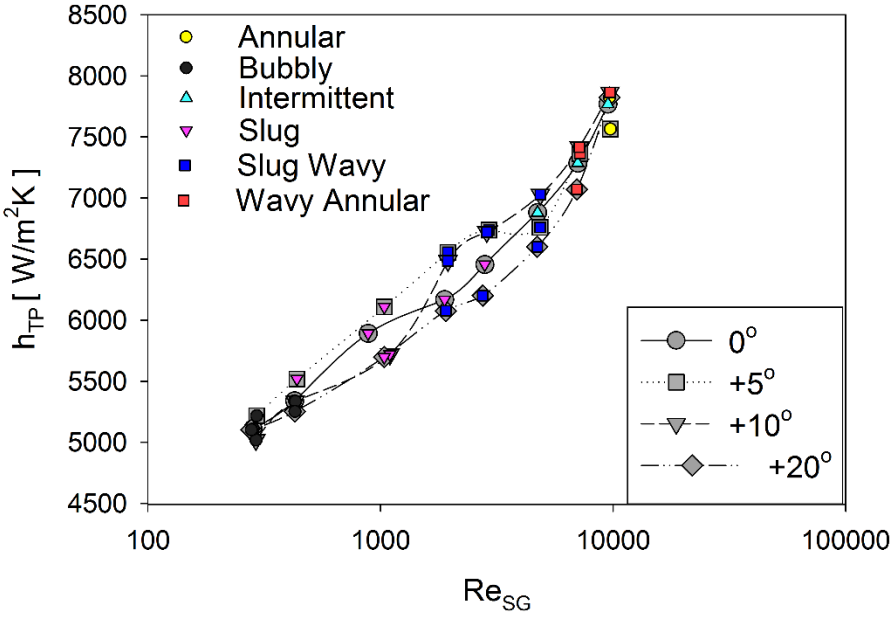

(c) Re_{SL} = 10,600

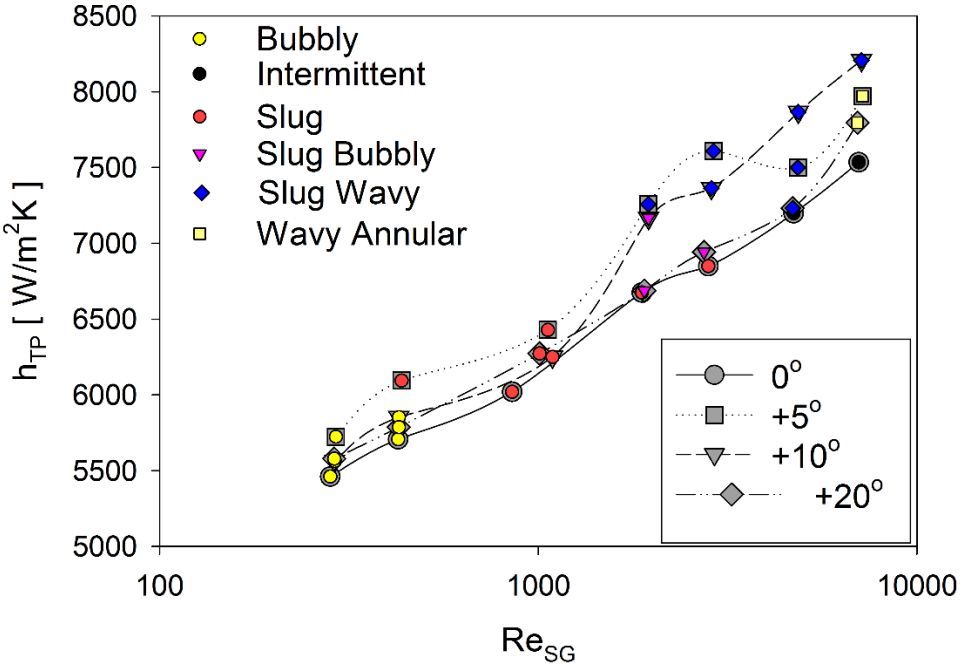

(d) Re_{SL} = 12,000

Figure 4.7 Comparison of two phase heat transfer coefficient at different liquid superficial Reynolds numbers for inclinations 0°, +5°, +10° and +20°.

With increasing liquid flow rates it is found that the two phase heat transfer coefficient in inclined system supersedes the h_{TP} in horizontal orientation to a greater degree. This is mostly because that at high liquid flow rates, the translational velocity of the gas slugs (in slug and wavy slug flow) or disturbance waves (in wavy annular and annular flow) is aided by the buoyancy acting on the gas phase that increases the slug/disturbance wave frequency and hence enhances two phase heat transfer coefficient with increase in the pipe orientation. However, it is found that at $+20^o$ pipe orientation, h_{TP} is consistently less than that observed in $+10^o$ inclination.

In order to verify if the two phase heat transfer coefficient decreases consistently between $+10^o$ and $+20^o$, some measurements are also carried out at an intermediate orientation of $+15^o$. These data points populated in +15° revealed that the heat transfer coefficient is maximum at +10° and from there on decreases with further increase in the pipe orientation. This can be attributed to the fact that as the inclination increases above +10° gravitational effects dominate the buoyancy effects to decrease the heat transfer. The phenomenon of waves creating instabilities in the heat transfer in upward inclinations can be also be attributed to the fact of 'wave undercutting'. This can be seen in **Figure 4.8.**

Conclusively, it can be said that for low liquid flow rates involving slug/slug wavy flow for +5° is predominantly greater than horizontal, $+10^o$ and $+20^o$. For medium liquid and gas flow rates with wavy and wavy annular two phase flow, heat transfer coefficient in $+10^o$ is greater than all the orientations considered in this study. For medium to high liquid flow rates ($7000 < Re_{SL} < 13000$), and all gas flow rates h_{TP} increases from 0^o to $+5^o$ and then from $+5^o$ to $+10^o$ and eventually decreases from $+10^o$ to $+20^o$.

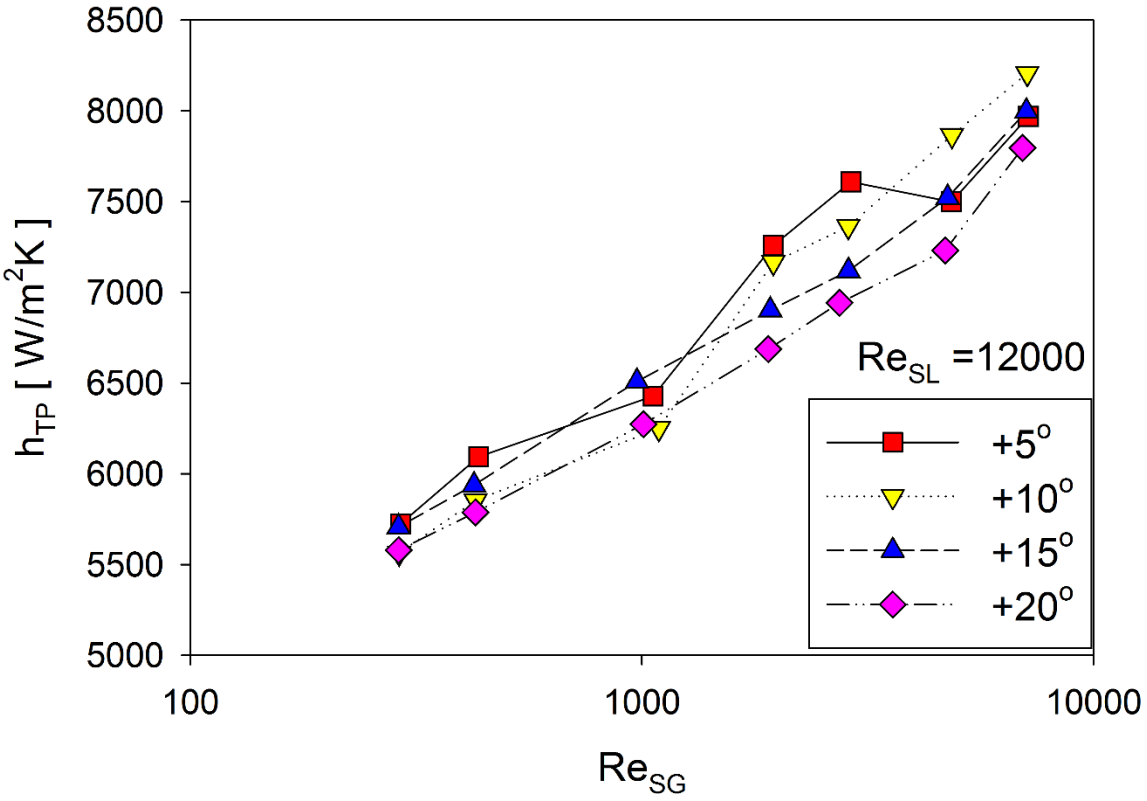

Figure 4.8 Comparison of h_{TP} among upward inclined pipe orientations

Incidentally, while conducting experiments in downward inclinations, Hossainy (2014) observed a decrease in heat transfer coefficient as the inclination progresses in the downward direction. This was attributed to the fact that the buoyancy always acts opposite to the direction of the liquid flow and the flow stratification in downward inclination. So, it can be summed up by the fact that in inclined flows (upward or downward), the increase/decrease of heat transfer coefficient for near horizontal inclinations is a contest between buoyancy and gravitational force. In upward inclination, an increase of heat transfer to certain inclination of + 10° is observed as the buoyancy overcomes the gravitational forces with high liquid flow rates. Thereafter, gravity overwhelms the buoyancy effect and starts to decrease. But, in downward flow the orientation of pipe facilitates for high liquid discharge, but encounters great resistance from the gas trying to move upwards.

It should also be noted that heat transfer experimentation is associated with certain uncertainty. This uncertainty in heat transfer experimentation is shown in Appendix - A.

4.4 Performance of the Heat Transfer Correlations

Correlations were developed by investigators to predict the heat transfer in two-phase flow. The results obtained by the current experimental data are compared with the results obtained by correlations available in the literature. The accuracy of the predicted points are measured in terms of percentage error, which is calculated as,

$$Error\ [\%] = \frac{h_{TP,\,CAL} - h_{TP,\,EXP}}{h_{TP,\,EXP}} \times 100 \tag{4.3}$$

Ten best performed correlations have been analyzed from the ones mentioned in the literature and best performing correlation is recommended and tabulated in tables. **Table 4.1**, **Table 4.2**, **Table 4.3** and **Table 4.4** for 0°, +5°, +10° and +20° respectively. Of the ten correlations tabulated in the above mentioned tables, the best performing correlations are discussed and plotted.

It has been observed that correlations of Shah (1981), Knott et al. (1959), and Kim et al. (2000) performed best among all the correlations in all the inclinations and in all the flow patterns. Among all the correlations, Shah (1981) correlation predicts the 96% of the points within the range of ± 30% error and 80% of the points with in the accuracy of ± 20% in all inclinations. In horizontal orientation, Shah (1981) correlation predicts 90% of the data with an accuracy of ± 30% and 84% of the data within the range of ± 20%. This decrease in prediction of experimental results in horizontal orientation when compared to the overall prediction can be attributed to the presence of stratified flow in horizontal orientation. Stratified flow due to its flow physics becomes very difficult to predict with correlations. Hence we see a fall in prediction of experimental results that can be predicted by Shah (1981) in horizontal flow. In + 5° orientation, it predicts 97% of the data

within a range of ± 30% and predict 80% of the data ± 20%. In + 10° orientation Shah predicts 99% of the points within the range of ± 30% and 71% of the points with ± 20% accuracy and 97% of the points within the range of ± 30% and 84% of the points with ± 20% in + 20° orientation. The overall prediction of experimental result of Shah (1981) correlation can be seen in **Figure 4.9**.

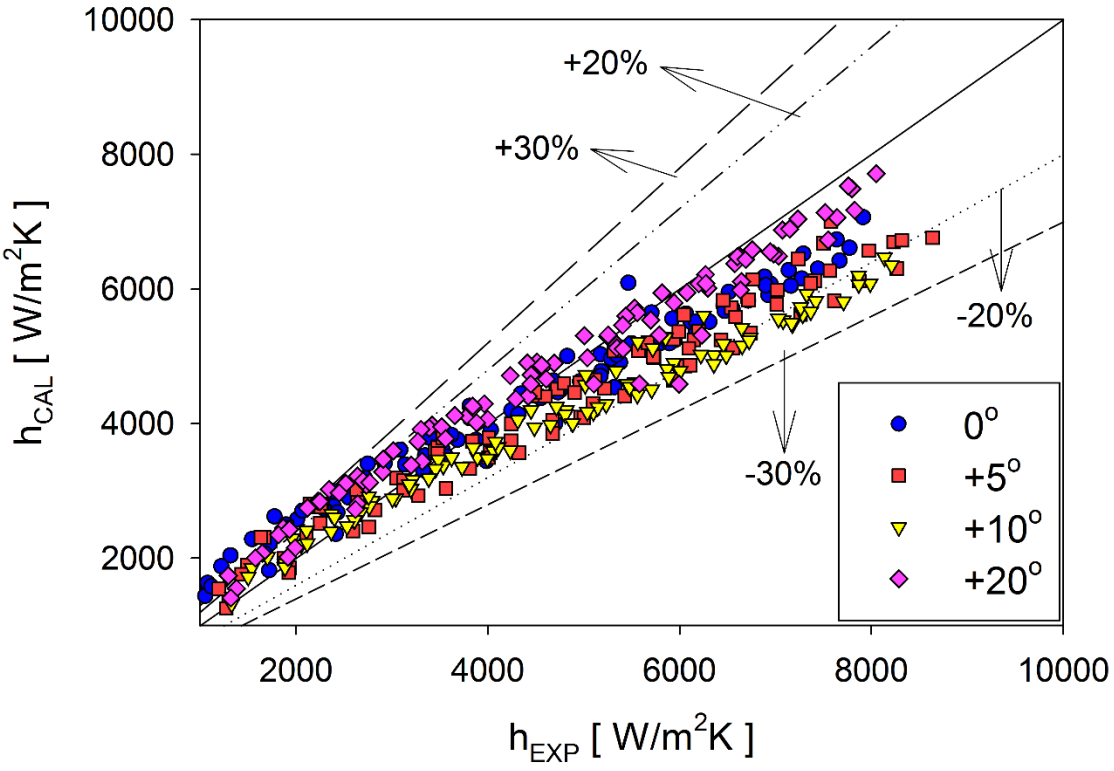

Figure 4.9 Experimental results' prediction by Shah (1981) correlation

Table 4.1 Performance of Correlations in 0°

Flow Pattern	90 (points)				S (24)		I (59)		St (5)		B (2)	
Correlations	**±30%**	**±20%**	**MabE**	**SD**	**±30%**	**±20%**	**±30%**	**±20%**	**±30%**	**±20%**	**±30%**	**±20%**
Aggour (1978)	**78**	**70**	10	24	63	71	81	86	0	0	50	100
Drucker et al. (1984)	**53**	**40**	25	22	92	96	17	34	60	80	100	100
Knott et al. (1959)	**68**	**61**	22	26	71	75	61	69	0	0	100	100
Shah (1981)	**90**	**84**	3	18	79	88	93	97	0	20	100	100
Martin and Sims (1971)	**18**	**8**	63	40	29	50	0	5	0	0	0	50
Kim et al. (2000)	**94**	**89**	5	19	79	88	100	100	0	60	100	100
Ravipudi and Godbold (1978)	**32**	**20**	69	68	46	63	12	24	0	0	50	50
Tang and Ghajar (2011)	**57**	**53**	30	31	0	0	78	81	40	60	0	0
Reynolds analogy correlations												
Vijay et al. (1982)	**80**	**49**	14	23	63	75	89	98	0	25	0	0
Bhagwat et al. (2012)	**85**	**74**	22	21	63	75	61	80	0	0	0	0

Prediction of data in the error band of ±30% and ±20%, MabE=Mean absolute error (%), SD= Standard deviation

Table 4.2 Performance of Correlations in +5°

Flow Pattern	95 points				A (29)		WA (11)		W (9)		SW (26)		S (17)		B (3)	
Correlations	**±30%**	**±20%**	**MabE**	**SD**	**±30%**	**±20%**	**±30%**	**±20%**	**±30%**	**±20%**	**±30%**	**±20%**	**±30%**	**±20%**	**±30%**	**±20%**
Aggour (1978)	**86**	**83**	7	19	86	86	82	82	78	78	77	88	88	88	100	100
Drucker et al. (1984)	**35**	**22**	34	14	0	0	0	0	0	11	19	46	76	100	100	100
Knott et al. (1959)	**79**	**72**	11	26	59	72	55	64	44	56	81	85	100	100	100	100
Shah (1981)	**97**	**80**	5	15	90	100	82	100	78	78	58	100	94	100	100	100
Martin and Sims (1971)	**38**	**27**	49	41	0	10	0	27	0	0	38	50	76	82	100	100
Kim et al. (2000)	**88**	**56**	15	11	14	93	45	100	100	100	62	100	94	100	100	100
Ravipudi and Godbold (1978)	**59**	**29**	34	20	52	86	82	100	44	100	0	42	0	0	0	0
Tang and Ghajar (2011)	**36**	**25**	52	65	7	14	18	27	0	0	46	58	47	71	0	0
Reynolds analogy correlations																
Vijay et al. (1982)	**56**	**48**	1	14	90	100	91	100	78	78	82	94	100	100	0	0
Bhagwat et al. (2012)	**95**	**88**	11	19	75	85	82	82	44	78	71	82	100	100	0	0

Prediction of data in the error band of ±30% and ±20%, MabE=Mean absolute error (%), SD= Standard deviation

Table 4.3 Performance of Correlations in +10°

Flow Pattern	90 points				A(26)		WA (14)		W (12)		SW (19)		S (13)		B (6)	
Correlations	**±30%**	**±20%**	**MabE**	**SD**	**±30%**	**±20%**	**±30%**	**±20%**	**±30%**	**±20%**	**±30%**	**±20%**	**±30%**	**±20%**	**±30%**	**±20%**
Aggour (1978)	**86**	**80**	8	22	73	85	86	86	75	83	74	84	85	85	67	100
Drucker et al. (1984)	**36**	**27**	35	18	0	0	0	0	0	25	26	53	100	100	100	100
Knott et al. (1959)	**86**	**81**	5	19	77	85	71	86	67	75	84	84	100	100	100	100
Shah (1981)	**99**	**31**	9	12	62	100	64	100	83	100	58	95	100	100	100	100
Martin and Sims (1971)	**50**	**27**	41	30	0	67	21	50	8	33	53	58	23	62	100	100
Kim et al. (2000)	**84**	**50**	17	13	4	46	21	100	92	100	58	100	100	100	100	100
Ravipudi and Godbold (1978)	**50**	**34**	44	52	8	31	36	6	17	25	58	12	62	69	33	100
Tang and Ghajar (2011)	**56**	**43**	36	28	88	96	79	100	25	67	0	16	0	0	0	0
Reynolds analogy correlations																
Vijay et al. (1982)	**79**	**70**	1	16	69	100	100	100	80	90	60	60	100	100	100	100
Bhagwat et al. (2012)	**90**	**75**	8	20	81	94	86	100	40	70	60	60	89	100	100	100

Prediction of data in the error band of ±30% and ±20%, MabE=Mean absolute error (%), SD= Standard deviation

Table 4.4 Performance of Correlations in +20°

Flow Pattern	95 points				A (30)		WA (11)		W (12)		SW (16)		S (13)		SB (4)		B (9)	
Correlations	±30%	±20%	MabE	SD	±30%	±20%	±30%	±20%	±30%	±20%	±30%	±20%	±30%	±20%	±30%	±20%	±30%	±20%
Aggour (1978)	**90**	**73**	9	19	90	90	82	91	25	67	56	88	62	100	100	100	100	100
Drucker et al. (1984)	**62**	**47**	24	20	0	3	0	36	50	100	81	100	100	100	100	100	100	100
Knott et al. (1959)	**66**	**53**	27	21	37	50	27	55	0	17	69	88	92	100	100	100	100	100
Shah (1981)	**97**	**84**	5	12	87	100	82	100	58	100	88	94	100	100	100	100	100	100
Martin and Sims (1971)	**2**	**1**	68	35	0	0	0	0	0	0	0	0	0	0	0	0	0	56
Kim et al. (2000)	**95**	**77**	5	14	37	83	100	100	92	100	88	100	100	100	100	100	100	100
Ravipudi and Godbold (1978)	**30**	**20**	69	61	0	3	0	9	0	0	13	31	46	62	100	100	78	100
Tang and Ghajar (2011)	**2**	**0**	66	25	0	0	0	18	0	0	0	0	0	0	0	0	0	0
Reynolds analogy correlations																		
Vijay et al. (1982)	**80**	**54**	10	15	96	100	91	91	25	58	100	100	100	100	100	100	100	100
Bhagwat et al. (2012)	**67**	**52**	24	19	64	79	36	55	0	17	86	100	100	100	100	100	100	100

Prediction of data in the error band of ±30% and ±20, MabE=Mean absolute error (%), SD= Standard deviation

Knott et al. (1959) correlation predicts 75% of the data for all inclinations within ± 30% range and 66% within ± 20% range. In horizontal orientation it predicts 68% of the data within ± 30% range and 61% of the data within ± 20%. In + 5° orientation 79% of the data within ± 30% range and 72% within ± 20% range. In + 10° orientation Knott's correlation predicts 86% of the data within ± 30% range and 81% in ± 20% range. In + 20° orientation the correlation predicts 66% of data in the range of ± 30% and 53% of the data in the range of ± 20%. The overall prediction of the correlation can be shown in **Figure 4.10**.

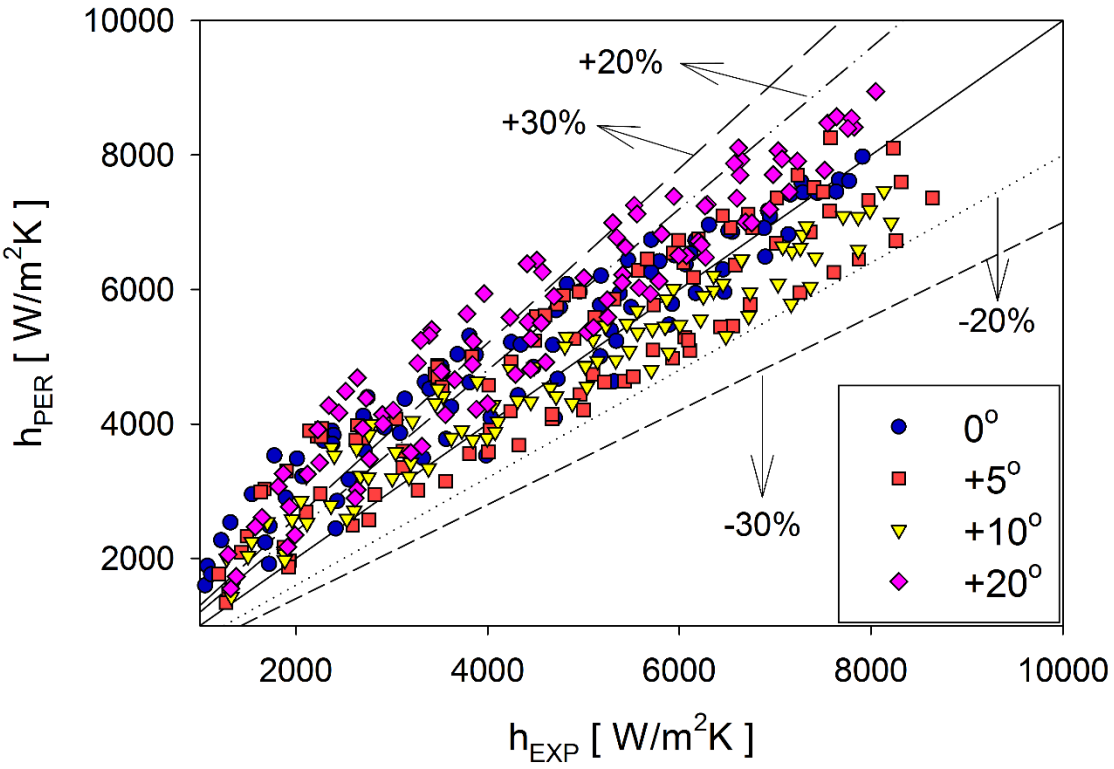

Figure 4.10 Experimental results' prediction by Knott et al. (1959) correlation

Kim et al. (2000) correlation predicts 93% of the data for all the inclinations within ± 30% range and 62% within ± 20% range. In horizontal orientation it correlation predicts 94% of the data within

± 30% range and 89% of the data within ± 20%. In + 5° orientation, the prediction is 88% of the data within ± 30% range and 56% within ± 20% range. In + 10° orientation the correlation predicts 84% of the data within ± 30% range and 50% in ± 20% range. In + 20° orientation the correlation predicts 95% of data in the range of ± 30% and 77% of the data in the range of ± 20%. The overall prediction of the correlation can be seen in **Figure 4.11**.

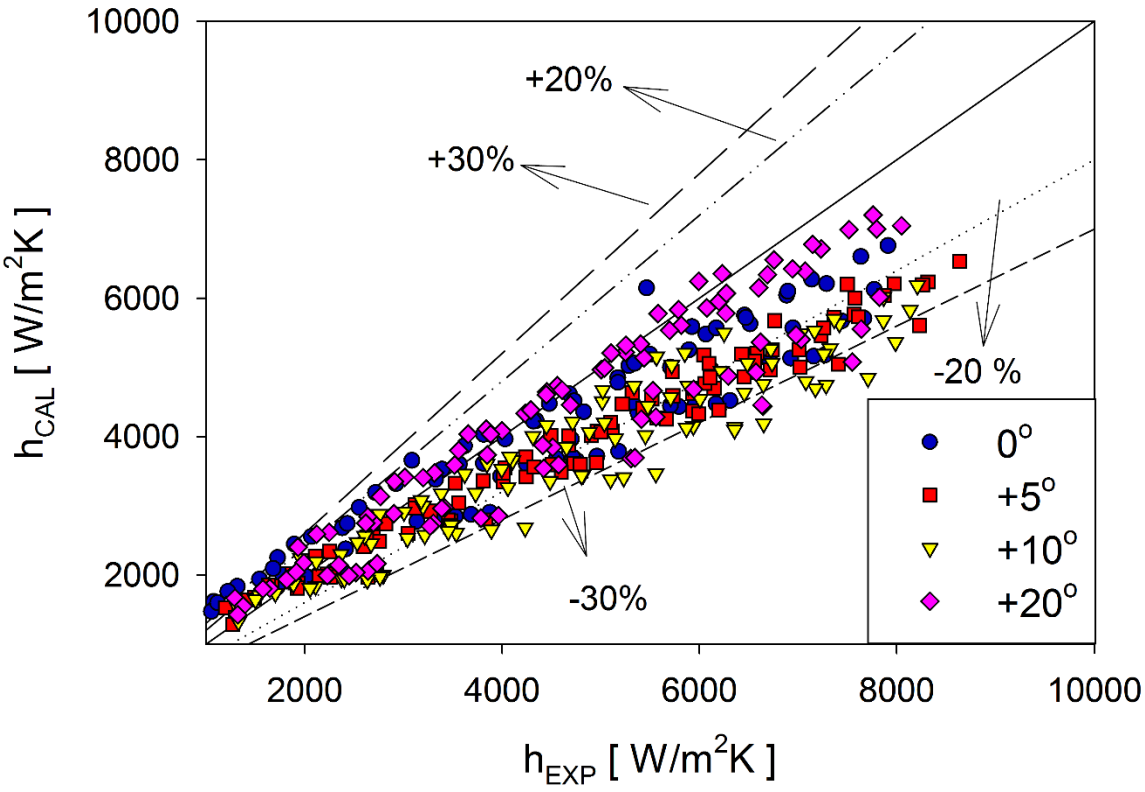

Figure 4.11 Experimental results' prediction by Kim et al. (2000) correlation

It is interesting to note that Kim et al. (2000) correlation predicts most of the data for all inclinations in wavy-annular and wavy regimes. In the upward inclined orientations involving wavy regime namely, wavy, wavy-annular and slug wavy the correlation predicts 100% of the data in ± 30% error band but decreases to 45% of prediction of data in wavy-annular regime but increases to

nearly 90% prediction in the range of ±20% in the flow regimes involving wavy flow other than wavy-annular.

Also, in general heat transfer correlations, Aggour (1978) predicts 85% of the data within ± 30% and 75% of the data within the range of ± 20% error. Also in inclinations less than + 20° the correlation predicts most of the data with about 80% of the data within the above mentioned error ranges.

Correlations have also been formed combining pressure drop and heat transfer using the principle of Reynolds analogy. For current experiments, to analyze correlations involving Reynolds analogy, isothermal pressure drop data has been obtained from Ghajar and Bhagwat (2014 b). Vijay et al. (1982) correlation and Bhagwat et al. (2012) correlation predicted most of the experimental data with Bhagwat et al. (2012) correlation performing better than Vijay et al. (1982) in correlations involving the principle of Reynolds analogy.

Vijay et al. (1982) correlation predicts 73% of the data within the range of ± 30% and 59% of the data in the range of ± 20% error including all orientations. In 0° it predicts 80% of the data within the range of ± 30% and 49% of the data in the range of ± 20%. In + 5° orientation the prediction is 56% of the data within ± 30% and 48% of the data in the range of ± 20% range. In +10° orientation it predicts 79% of the data within ± 30% range and 70% of the data in ± 20% range. In +20° orientation it predicts 80% of the data in ± 30% range and 54% of the data in ± 20%.

Bhagwat et al. (2012) correlation predicts 78% of the data within the range of ± 30% and 64% of the data in the range of ± 20% error including all orientations. In 0° it predicts 85% of the data within the range of ± 30% and 74% of the data in the range of ± 20%. In + 5° orientation the prediction is 95% of the data within ± 30% and 88% of the data in the range of ± 20% range. In +10° orientation it predicts 90% of the data within ± 30% range and 75% of the data in ± 20% range. In + 20° orientation it predicts 67% of the data in ± 30% range and 52% of the data in ± 20%.

The Reynolds analogy correlations mentioned above are compared and plotted as shown in **Figure 4.12**. The performance of Bhagwat et al. (2012) correlation is found to be better than Vijay (1982) correlation. Modification to Vijay et al. (1982) correlation is suggested to make it best performing Reynolds analogy correlation.

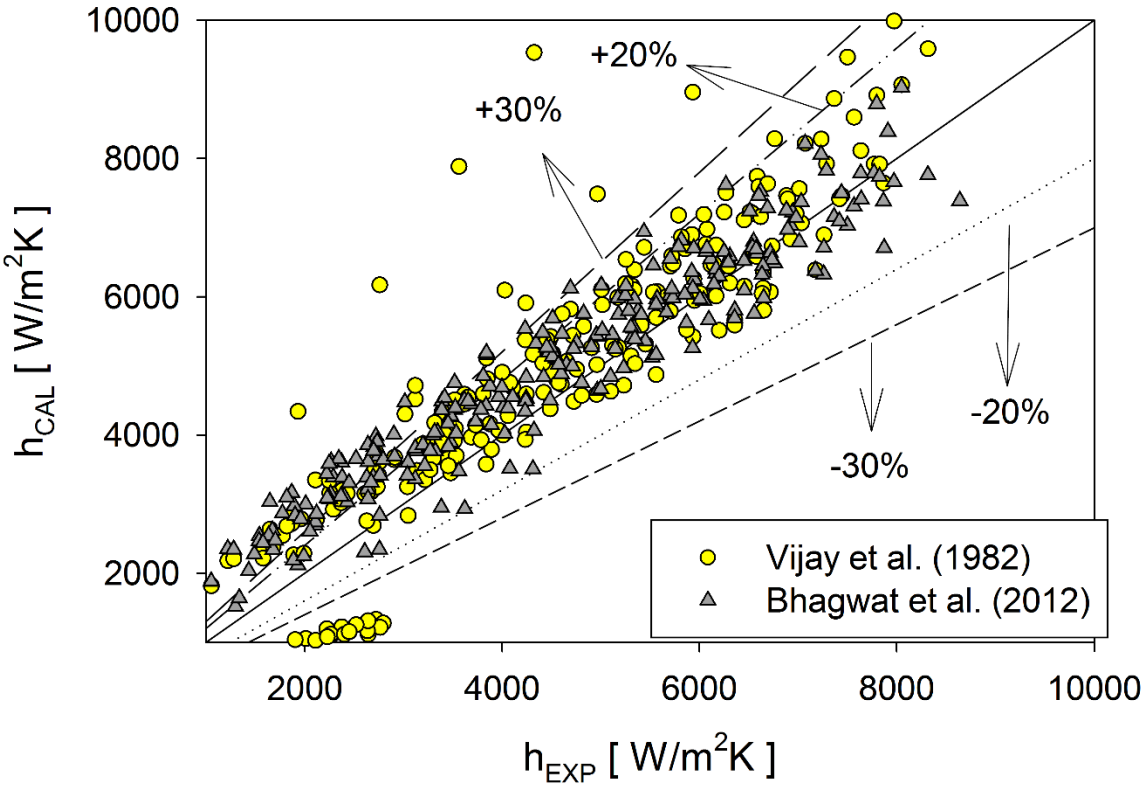

Figure 4.12 Performance of Reynolds analogy correlations

Heat Transfer Correlation modification

Vijay et al. (1982) correlation is chosen to modify to predict the experimental data. This is because the best performing correlation using Reynolds analogy Bhagwat et al. (2012) was modified from the Vijay et al. (1982) correlation.

Vijay et al. (1982) correlation is given by the form

$$h_{TP}/h_L = \left(\Delta p_{TPf}/\Delta p_L \right)^{0.451} \tag{4.4}$$

where

$$Nu_L = 1.615\left[\mathrm{Re}_{SL}\, \mathrm{Pr}_L \left(D/L \right) \right]^{1/3} \left(\mu_B/\mu_W \right)^{0.14} \quad \text{(L)} \tag{4.5}$$

$$Nu_L = 0.0155\, \mathrm{Re}_{SL}{}^{0.83}\, \mathrm{Pr}_L{}^{0.5} \left(\mu_B/\mu_W \right)^{0.33} \quad \text{(T)} \tag{4.6}$$

The above mentioned correlation is modified for better results and analysis of the data. The modification of the Vijay et al. (1982) correlation is of the form

$$h_{TP}/h_L = \left(\Delta p_{TPf}/\Delta p_L \right)^{0.39} \tag{4.7}$$

where

$$Nu_L = 1.86\left[\mathrm{Re}_{SL}\, \mathrm{Pr}_L \left(D/L \right) \right]^{1/3} \left(\mu_B/\mu_W \right)^{0.14} \quad \text{(L)} \tag{4.8}$$

$$Nu_L = 0.027\, \mathrm{Re}_{SL}{}^{0.83}\, \mathrm{Pr}_L{}^{0.5} \left(\mu_B/\mu_W \right)^{0.33} \quad \text{(T)} \tag{4.9}$$

Equations (4.8) and (4.9) are taken from the Sieder and Tate (1936) single phase heat transfer correlation and are used to modify Vijay et al. (1982) correlation to get the best performing correlation for the data in upward inclined orientation. It is also important to note that the proposed correlation varies with Bhagwat et al. (2012) correlation only in the index of the dimensionless pressure drop parameter. The form and structure of the proposed correlation remains same as that of Bhagwat et al. (2012) correlation.

The modified Vijay et al. (1982) correlation predicts 97% of the data in all orientations in ± 30% range and 82% of the data in ± 20% range. In + 5° orientation the prediction is 100% of the data in ± 30% range and 80% of the points in ± 20% range. In + 10° orientation the prediction is 100% of the data in ± 30% range and 71% of the points in ± 20% range and 84% of the points in ± 25% range. In + 20° orientation the prediction is 100% of the data in ± 30% range and predicts 90% of the data in ± 20% range. The modified Vijay et al. (1982) correlation can be seen in **Figure 4.13**. This modification of the Vijay et al. (1982) correlation predicts most of the data.

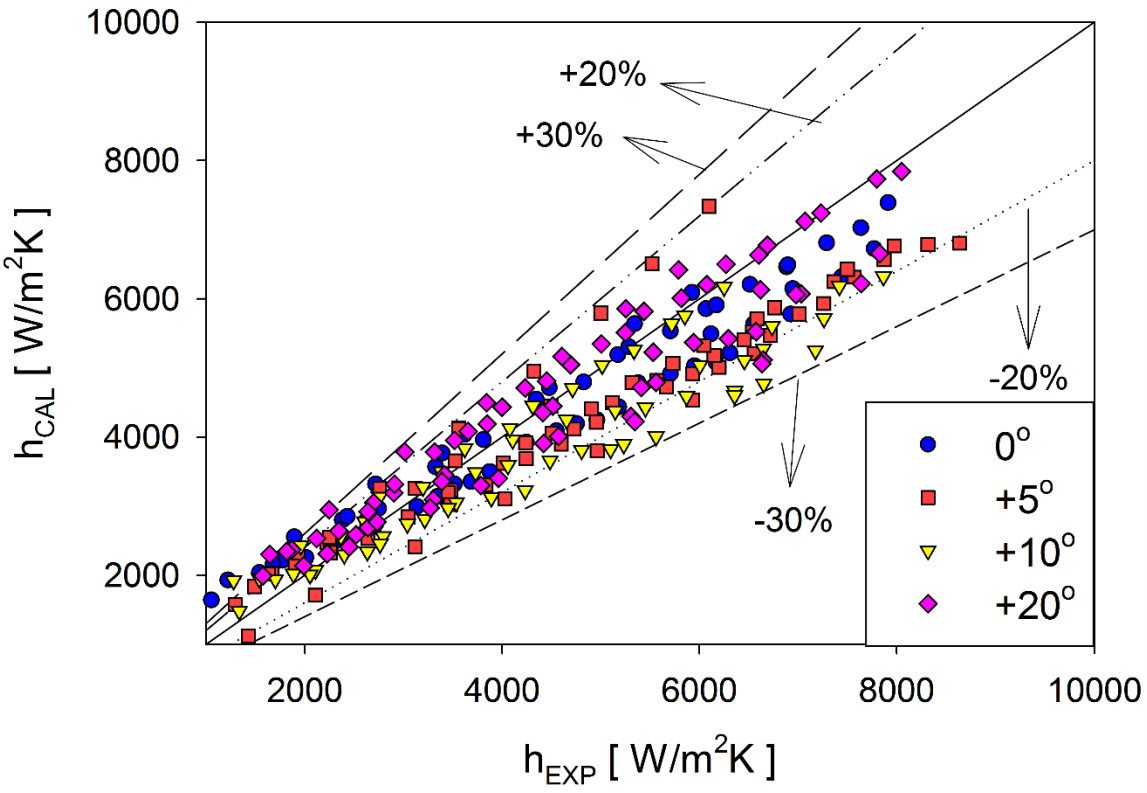

Figure 4.13 Performance of proposed correlation

Now, the comparison between proposed (modified Vijay et al. (1982)) correlation and Bhagwat et al. (2012) correlation is shown in **Figure 4.14**.

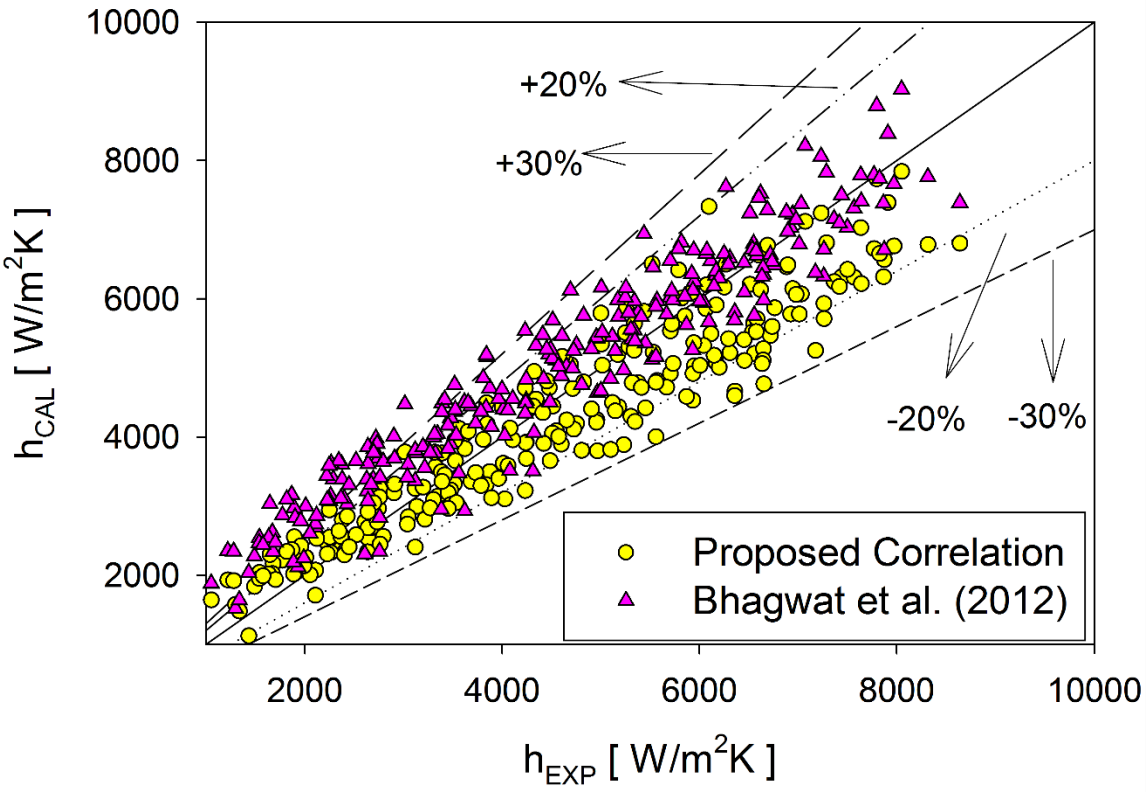

Figure 4.14 Performance of proposed and Bhagwat et al. (2012) correlations.

Based on the performance of the correlations it is evident that the proposed correlation performs the best amongst the Reynolds analogy correlations. This is also observed in downward inclination flow when modification of Vijay et al. (1982) correlation is suggested by Hossainy (2014) for downward inclination data. Hossainy (2014) observed that Shah (1981) performs best in the general heat transfer correlations for downward near horizontal inclined correlations.

CHAPTER V

SUMMARY, CONCLUSIONS AND RECOMMENDATIONS

The conclusions obtained by the current study establishes the fundamental understanding of the heat transfer in upward inclination and the effect of flow pattern and inclination on the heat transfer coefficient in two phase flow. The pressure drop data obtained by Ghajar and Bhagwat (2014 b) is used to develop a Reynolds analogy correlation along with the heat transfer data.

From the results the following conclusions are evident

1. The two phase heat transfer coefficient in upward inclination is heavily dependent on the flow pattern. In the slug-wavy flow regime, which is an intermittent form of the slug flow, the heat transfer coefficient in +5° surpasses heat transfer coefficient in +10°.This is due to the repeated wetting of the top surface in the slug-wavy region which is evident from the magnitude of peripheral heat transfer coefficients observed in different flow regimes. But, while taking the total heat transfer data collected into picture, it can be concluded that the heat transfer is maximum in +10°. The heat transfer coefficient increases from +5° to +10° and then starts to decrease from +10° to +20°. This fact is clearly evident by the data collected in +15° where the heat transfer coefficient is observed to be decreasing than that of +10°.
2. This increase of heat transfer from +5° to +10° can be attributed to the buoyancy effects of the gas phase, where the gas phase tends to push the liquid phase upward increasing the heat transfer coefficient in the orientation.

3. From +10° to +20° the heat transfer coefficient decreases due to the domination of gravitational forces at higher inclinations.
4. The heat transfer dependence on the two phase flow in upward inclination dependence can be defined as the contest between gravitational and buoyance forces for near horizontal inclinations.
5. In flow reversal region the heat transfer analysis becomes unpredictable and unreliable due to the chaotic nature of the flow.
6. Correlations were compared and Shah (1981) correlation was found to be the best correlation in general heat transfer correlation category. In Reynolds analogy correlations Vijay et al. (1982) correlation and Bhagwat et al. (2012) correlation have found to be doing better and Bhagwat etal. (2012) correlation performs best in the two.
7. Vijay et al. (1982) correlation was modified to get the best correlation to predict the experimental heat transfer data in upward inclination of two-phase flow. This correlation is chosen because Bhagwat et al. (2012) correlation was also developed from Vijay et al. (1982) correlation.

Recommendations for future work

1. It would interesting to know the effect on heat transfer coefficients for different diameters, other inclinations and various fluid combinations. This opens new avenues in the field of two-phase heat transfer to see whether the flow physics and heat transfer changes predictably.
2. It would also be interesting to study the heat transfer in flow reversal region in detail to get the understanding of the heat transfer coefficient behavior in the flow reversal region.

REFERENCES

Aggour, M. A. (1978). *Hydrodynamics and Heat Transfer in Two-Phase Two-Component Flow.* (Ph.D. Dissertation), University of Manitoba, Canada.

Bhagwat, S. M., Mollamahmutoglu, M., & Ghajar, A. J. (2012). *Experimental Investigation and Empirical Analysis of Non-boiling Gas-liquid Two Phase Heat Transfer in Vertical Downward Pipe Orientation.* Paper presented at the Proceedings of ASME 2012 Summer Heat Transfer Conference (HT2012), Puerto Rico.

Carey, V. A. (1992). *Liquid-Vapor Phase-Change Phenomena: An Introduction to the Thermophysics of Vaporization and Condensation Process in Heat Transfer Equipment*. Bristol, U.K.: Taylor and Francis.

Cook, W. (2008). *An Experimental Apparatus for Measurement of Pressure Drop, Void Fraction, and Non-boiling Two-phase Heat transfer and Flow Visualization in Pipes for All Inclinations.* (Master of Science), Oklahoma State University, Stillwater, OK.

Deshpande, S. D., Bishop, A. A., & Mkrandikar, B. M. (1991). Heat Transfer to Air-Water Plug-Slug Flow in Horizontal Pipes. *I&EC Research, 30,* 2172–2180.

DiMarco, P., Kim, J., & Ohta, H. (2009). Boiling Heat Transfer in Reduced Gravity Environments. In L. Cheng & D. Mewes (Eds.), *Advances in Multiphase Flow and Heat Transfer* (Vol. 1, pp. 53-92). UK: Bentham Sciences Publisher.

Fogler, H. S. (2008, Nov. 25, 2008). Paraffin Research. *Porous Media Research Group.* from sitemaker.umich.edu/sfogler/paraffin_deposition

Fried, L. (1954). Pressure Drop and Heat Transfer for Two-Phase, Two-Component Flow. *Chem. Eng. Prog. Symp. Series, 50*(9), 47–51.

Ghajar, A., & Kim, J. (2006). Calculation of Local Inside-Wall Convective Heat Transfer Parameters from Measurements of the Local Outside-Wall Temperatures along an Electrically Heated Circular Tube. In M. Kutz (Ed.), *Heat Transfer Calculations* (pp. 23.23-23.27). NewYork, NY: Mc-Graw-Hill.

Ghajar, A. J., & Bhagwat, S. M. (2014a). A Flow Pattern Independent Drift Flux Model Based Void Fraction Correlation for a Wide Range of Gas-Liquid Two Phase Flow. *International Journal of Multiphase Flow, 59*, 186-205.

Ghajar, A. J., & Bhagwat, S. M. (2014b). Gas-Liquid Two Phase Flow Phenomenon in Near Horizontal Upward and Downward Inclined Pipe Orientations. *International Journal of Mechanical, Aerospace, Industrial and Mechatronics Engineering, 8*(6), 1039-1053.

Ghajar, A. J., & Tam, L. M. (1994). Heat Transfer Measurements and Correlations in the Transition Region for a Circular Tube with Three Different Inlet Configurations, Experimental Thermal and Fluid Science. *8*, 79-90.

Gnielinski, V. (1976). New Equations for Heat and Mass Transfer in Turbulent Pipe and Channel Flows. *Int. Chemical Engineering, 16*, 359-368.

Hetsroni, G., Hu, B. G., Yi, B. G., Mosyak, A., Yarin, L. P., & Ziskind, G. (1998a). Heat Transfer in Intermittent Air-Water Flow–Part I: Horizontal Tube. *Int. J. Multiphase Flow, 24*(2), 165–188.

Hetsroni, G., Hu, B. G., Yi, B. G., Mosyak, A., Yarin, L. P., & Ziskind, G. (1998b). Heat Transfer in Intermittent Air-Water Flow, Part II: Upward Inclined Tube. *Int. J. Multiphase Flow, 24*, 188–212.

Hossainy, T. A. (2014). *Non-Boiling Heat Transfer In Horizontal And Near Horizontal Downward Inclined Gas-Liquid Two Phase Flow.* Master's Thesis. Mechanical and Aerospace Engineering. Oklahoma State University. Stillwater, OK.

Hughmark, G. A. (1965). Holdup and Heat Transfer in Horizontal Slug Gas-Liquid Flow. *Chem. Eng. Sci., 20*, 1007-1010.

Johnson, H. A., & Abou-Sabe, A. H. (1952). Heat Transfer and Pressure Drop for Turbulent Flow of Air-Water Mixture in a Horizontal Pipe. *Trans. ASME, 50*(9), 47–51.

Julia, J. E., Hibiki, T., & Ishii, M. (2009). Two-Phase Flow Regime Identification Methodologies in Thermal-Hydraulic Applications. In L. Cheng & D. Mewes (Eds.), *Advances in Multiphase Flow and Heat Transfer* (Vol. 1, pp. 93-112). UK: Bentham Sciences Publisher.

Kim, Ghajar, A. J., & Dougherty, R. L. (2000). Robust Heat Transfer Correlation for Turbulent Gas-Liquid Flow in Vertical Pipes. *Journal of Thermophysics and Heat Transfer, 14*(4), 574-578.

Kim, D. (2000). *An Experimental and Empirical Investigation of Convective Heat Transfer for Gas-Liquid Two-Phase Flow in Vertical and Horizontal Pipes.* (Ph.D.), Oklahoma State University, Stillwater, OK.

Kim, J., & Ghajar, A. J. (2006). A General Heat Transfer Correlation for Non-Boiling Gas-Liquid Flow with Different Flow Patterns in Horizontal Pipes. *Int. J. Multiphase Flow, 32*, 447–465.

King, C. D. G. (1952). *Heat Transfer and Pressure Drop for an Air-Water Mixture Flowing in a 0.737 inch I.D. Horizontal Tube.* (Master of Science), University of California, Berkeley, CA.

Kline, S. J., & McClintock, F. A. (1953). Describing Uncertainties in Single Sample Experiments. *Mechanical Engineering, 1*, 3-8.

Knott, R. F., Anderson, R. N., Acrivos, A., & Petersen, E. E. (1959). An Experimental Study of Heat Transfer to Nitrogen-Oil Mixtures. *Industrial and Engineering Chemistry, 51*(11), 1369-1372.

Kroes, J. P., Geld, C. W. M. v. d., & Velthooven, E. v. (2009). Evaluation of Four Nucleate Flow Boiling Models. In L. Cheng & D. Mewes (Eds.), *Advances in Multiphase Flow and Heat Transfer.* (Vol. 1, pp. 267-283). UK: Bentham Sciences Publisher.

Lockhart, R. W., & Martinelli, R. C. (1949). Proposed Correlation of Data for Isothermal Two-Phase, Two-Component Flow in Pipes. *Chemical Engineering Process, 45*(1), 39–48.

Martin, B. W., & Sims, G. E. (1971). Forced Convection Heat Transfer to Water with Air Injection in a Rectangular Duct. *I&EC Fundamentals, 14*, 1115–1134.

Oliver, D. R., & Wright, S. J. (1964). Pressure Drop and Heat Transfer in Gas-Liquid Slug Flow in Horizontal Tubes. *British Chemical Engineering, 9*, 590-596.

Oyewole, A. (2013). *Study Of Flow Patterns And Void Fraction In Inclined Two Phase Flow.* (Master of Science), Oklahoma State University, Stillwater.

Sardeshpande, M. V., & Ranade, V. V. (2013). Two-phase flow boiling in small channels: A brief review. *Sadhana, 38*(6), 1083-1126.

Shah, M. M. (1981). Generalized Prediciton of Heat Transfer during Two-Component Gas-Liquid Flow in Tubes and Other Channels. *AIChE Symp. Series, 77*, 140-151.

Shoham, O., Dukler, A. E., & Taitel, Y. (1982). Heat transfer during intermittent/slug flow in horizontal tubes. *Industrial & Engineering Chemistry Fundamentals, 21*(3), 312-319. doi: 10.1021/i100007a020

Sieder, E. N., & Tate, G. E. (1936). Heat Transfer and Pressure Drop of Liquids in Tubes. *Industrial and Engineering Chemistry, 28*, 1429-1435.

Singh, P., Venkatesan, R., Fogler, H. S., & Nagarajan, N. (2000). Formation and Aging of Incipient Thin Film Wax-Oil Gels. *AIChE Journal, 46*(5), 1059-1074.

Smith, S. L. (1969). Void Fraction in Two Phase Flow: A Correlation Based upon an Equal Velocity Head Model. *Proc. Inst. Mech. Engrs, London., 184*, 647-657.

Taitel, Y., & Dukler, A. E. (1976). A Model For Predicting Flow Regime Transitions in Horizontal and Near Horizontal Gas-Liquid Flow. *American Institute of Chemical Engineers, 22*(1), 47-55.

Tang, C. C. (2011). *A Study Of Heat Transfer In Non-Boiling Two-Phase Gas-Liquid Flow In Pipes For Horizontal, Slightly Inclined, And Vertical Orientations.* (Ph.D.), Oklahoma State University, Stillwater, Oklahoma.

Tang, C. C., & Ghajar, A. J. (2011). A Mechanistic Heat Transfer Correlation for Non-Boiling Two-Phase Flow in Horizontal, Inclined and Vertical Pipes *Proceedings of ASME/JSME 2011(AJTE2011) 8th Thermal Engineering Joint Conference*. Honolulu, Hawaii.

Vijay, M. M., Aggour, M. A., & Sims, G. E. (1982). *A Correlation of Mean Heat Transfer Coefficients for Two-Phase Two-Component Flow in a Vertical Tube.* Paper presented at the Proceedings of the 7th International Heat Transfer Conference, Munich, Germany.

Woldesemayat, M. A., & Ghajar, A. J. (2007). Comparison of Void Fraction Correlations for Different Flow Patterns in Horizontal and Upward Inclined Pipes. *International Journal of Multiphase Flow, 33*(4), 347-370.

APPENDIX - A

UNCERTAINTY ANALYSIS

In this study the uncertainty of the measured parameters is calculated. The parameters that are involved in the study were non-isothermal pressure drop and heat transfer coefficient. The uncertainty pertaining to each of the parameters have been investigated using the methods proposed by Kline and McClintock (1953).

$$w_R = \left(\left(\frac{\partial R}{\partial x_1} w_1 \right)^2 + \left(\frac{\partial R}{\partial x_2} w_2 \right)^2 + \left(\frac{\partial R}{\partial x_3} w_3 \right)^2 + \ldots\ldots + \left(\frac{\partial R}{\partial x_n} w_n \right)^2 \right)^{\frac{1}{2}} \tag{A.1}$$

Heat Transfer

Nusselt number is used as the criterion to calculate the heat transfer in the experiment.

The heat transfer coefficient is given by

$$h = \frac{\dot{q}''}{\overline{T}_{wi} - \overline{T}_b} = \frac{\dot{q}''}{\Delta T} \tag{A.2}$$

The uncertainty for the heat transfer coefficient using Kline and McClintock (1953) can be written as

$$w_h = \left[\left(\frac{\partial h}{\partial \dot{q}''} w_{\dot{q}''} \right)^2 + \left(\frac{\partial h}{\partial \Delta T} w_{\Delta T} \right)^2 \right]^{\frac{1}{2}}$$

$$w_h = \left[\left(\frac{1}{\Delta T} w_{\dot{q}''} \right)^2 + \left(\frac{-\dot{q}''}{\Delta T} w_{\Delta T} \right)^2 \right]^{\frac{1}{2}} \tag{A.3}$$

It is clear that the calculation of heat transfer coefficient depends on the inner wall temperature (T_{wi}) and bulk temperature (T_B).

The inner wall temperature is given by

$$\bar{T}_{wi} = \dot{q}R_t + \bar{T}_{wo} \tag{A.4}$$

The uncertainty associated with the inner wall temperature is calculated by

$$w_{\bar{T}_{wi}} = \left[\left(\frac{\partial \bar{T}_{wi}}{\partial \dot{q}} w_{\dot{q}} \right)^2 + \left(\frac{\partial \bar{T}_{wi}}{\partial R_t} w_{R_t} \right)^2 + \left(\frac{\partial \bar{T}_{wi}}{\partial \bar{T}_{wo}} w_{\bar{T}_{wo}} \right)^2 \right]^{\frac{1}{2}}$$

Now, the uncertainty of the inner wall temperature is

$$w_{\bar{T}_{wi}} = \left[\left(R_t w_{\dot{q}} \right)^2 + \left(\dot{q} w_{R_t} \right)^2 + \left(w_{\bar{T}_{wo}} \right)^2 \right]^{\frac{1}{2}} \tag{A.5}$$

The inner wall and the outer wall temperatures are both averages. So, for the outer wall temperature, the average of all the four thermocouples in a station is taken and is given by

$$\bar{T}_{wosn} = \frac{\bar{T}_{wo-1} + \bar{T}_{wo-2} + \bar{T}_{wo-3} + \bar{T}_{wo-4}}{4} \tag{A.6}$$

In Eq. (A.6) T_{wosn} is the average outer wall temperature at the given station number. There are 7 stations along the length of the pipe to calculate the outer wall temperature. The uncertainty of the thermocouples attached to the pipe was calibrated to be $\pm$ 0.5°C. As uncertainty of the thermocouples are identical we can say that the uncertainty of each station is $\pm$0.5°C. The average of all the 7 stations is

$$\bar{T}_{wo} = \frac{\bar{T}_{wo-1} + \bar{T}_{wo-2} + \bar{T}_{wo-3} + \bar{T}_{wo-4} + \bar{T}_{wo-5} + \bar{T}_{wo-6} + \bar{T}_{wo-7}}{7} \tag{A.7}$$

As the uncertainty of each station is $\pm$0.5°C, the uncertainty of the average of all the stations is also $\pm$0.5°C.

It is also essential to calculate the uncertainty of the thermal resistance which is given by

$$R_t = \frac{\ln\left(D_o / D_i\right)}{2\pi kL} \tag{A.8}$$

Its uncertainty is

$$w_{R_t} = \left[\left(\frac{\partial R_t}{\partial D_o} w_{D_o}\right)^2 + \left(\frac{\partial R_t}{\partial D_i} w_{D_i}\right)^2 + \left(\frac{\partial R_t}{\partial k} w_k\right)^2 + \left(\frac{\partial R_t}{\partial L} w_L\right)^2\right]^{\frac{1}{2}}$$

which reduces to

$$w_{R_t} = \left[\left(\frac{1}{2\pi D_o kL} w_{D_o}\right)^2 + \left(\frac{-1}{2\pi D_i kL} w_{D_i}\right)^2 + \left(\frac{-\ln\left(D_o / D_i\right)}{2\pi k^2 L} w_k\right)^2 + \left(\frac{-\ln\left(D_o / D_i\right)}{2\pi L^2 k} w_L\right)^2\right]^{\frac{1}{2}}$$

(A.9)

It should be noted that the uncertainties involved in calculation of the thermal resistance are all standard uncertainties. So, the uncertainty calculated for the thermal resistance will be the standard uncertainty for the experiment.

It is also necessary to calculate the uncertainty of the heat transfer rate and also heat flux. The uncertainty of the heat transfer rate is given by

$$\dot{q} = V_D i \tag{A.10}$$

The uncertainty is

$$w_{\dot{q}} = \left[\left(\frac{\partial \dot{q}}{\partial V_D} w_{V_D}\right)^2 + \left(\frac{\partial \dot{q}}{\partial i} w_i\right)^2\right]^{\frac{1}{2}}$$

which is simplified to

$$w_{\dot{q}} = \left[\left(i w_{V_D}\right)^2 + \left(V_D w_i\right)^2\right]^{\frac{1}{2}} \tag{A.11}$$

Though heat transfer can be calculated using the enthalpy of the system, Eq. (A.7) is preferred for experimental and finite difference calculations. The heat transfer calculated through enthalpy is

$$\dot{q} = \dot{m}c\left(T_{B,out} - T_{B,in}\right) \tag{A.12}$$

From the experiment the heat balance error is obtained. The heat balance error is the difference between the heat transfer rate calculated through enthalpy and the power input to the experimental system. This error is added to the uncertainty to get maximum and minimum uncertainty for heat transfer calculation.

The heat flux of the system is given by

$$\dot{q}'' = \frac{V_D i}{\pi D_i L} \tag{A.13}$$

whose uncertainty is

$$w_{\dot{q}''} = \left[\left(\frac{\partial \dot{q}''}{\partial V_D} w_{V_D}\right)^2 + \left(\frac{\partial \dot{q}''}{\partial i} w_i\right)^2 + \left(\frac{\partial \dot{q}''}{\partial D_i} w_{D_i}\right)^2 + \left(\frac{\partial \dot{q}''}{\partial L} w_L\right)^2\right]^{\frac{1}{2}}$$

Which is simplified to

$$w_{\dot{q}''} = \left[\left(\frac{i}{\pi D_i L} w_{V_D}\right)^2 + \left(\frac{V_D}{\pi D_i L} w_i\right)^2 + \left(\frac{-V_D i}{\pi D^2{}_i L} w_{D_i}\right)^2 + \left(\frac{-V_D i}{\pi D_i L^2} w_L\right)^2\right]^{\frac{1}{2}} \tag{A.14}$$

The single phase uncertainty values' calculation for the heat transfer coefficient for best case and worst case are tabulated as shown in **Table A-1, Table A-2,** respectively**.**

The two phase uncertainty values' calculation for the heat transfer coefficient for worst case and best case are tabulated as shown in **Table A-3, Table A-4,** respectively.

Single phase uncertainty values sample calculation

Table A-1 Single Phase Uncertainty (Best Case RUN 0001)

Variable	Value	Uncertainty	Uncertainty %
Inner Diameter (D_i) (m)	0.0125	±1.270E-05	±0.1
Outer Diameter (D_o) (m)	0.0171	±1.270E-05	±0.07
Length (L) (m)	1.016	±3.175E-03	0.31
Thermal Conductivity (k) ($W/m\text{-}K$)	13.438	NA	NA
Ampere (i) (A)	579.2	±5.79	±1.00
Voltage (V_D) (V)	3.96	±0.0396	±1.00
Thermal Resistance (R_t) (K/W)	0.0036	±1.85E-5	±0.51
Average Inner Wall Temperature (T_{wi}) ($°C$)	31.05	±0.5	±1.48
$T_{wi} - T_B$ (ΔT) ($°C$)	17.55	±1.01	±5.6
Heat Transfer Rate ($\dot{q}$) (W)	2290.21	±32.43	±1.36
Heat Flux ($\dot{q}''$) (W/m^2)	57302.92	±833.50	±1.45
Heat Transfer Coefficient (h) ($W/m^2\text{-}K$)	7783.671	±413.206	±5.31

Table A-2 Single Phase Uncertainty (Worst case RUN 0018)

Variable	Value	Uncertainty	Uncertainty %
Inner Diameter (D_i) (m)	0.0125	±1.270E-05	±0.1
Outer Diameter (D_o) (m)	0.0171	±1.270E-05	±0.07
Length (L) (m)	1.016	±3.175E-03	0.31
Thermal Conductivity (k) ($W/m\text{-}K$)	13.438	NA	NA
Ampere (i) (A)	579.2	±5.79	±1.00
Voltage (V_D) (V)	3.96	±0.0396	±1.00
Thermal Resistance (R_t) (K/W)	0.0036	±1.85E-5	±0.51
Average Inner Wall Temperature (T_{wi}) ($°C$)	31.05	±0.5	±1.48
$T_{wi} - T_B$ (ΔT) ($°C$)	13.00	±1.01	±5.6
Heat Transfer Rate ($\dot{q}$) (W)	2310.21	±6.96	±1.36
Heat Flux ($\dot{q}''$) (W/m^2)	492.21	±833.50	±1.45
Heat Transfer Coefficient (h) ($W/m^2\text{-}K$)	596.1	±72.01	±12.08

Two phase uncertainty values sample calculation

Table A-3 Uncertainty Calculations Worst Case +5° (RUN 0001)

Variable	Value	Uncertainty	Uncertainty %
Inner Diameter (D_i) (m)	0.0125	±1.270E-05	±0.1
Outer Diameter (D_o) (m)	0.0171	±1.270E-05	±0.07
Length (L) (m)	1.016	±3.175E-03	0.31
Thermal Conductivity (k) ($W/m\text{-}K$)	13.438	NA	NA
Ampere (i) (A)	219.29	±2.19	±1.00
Voltage (V_D) (V)	1.71	±0.0171	±1.00
Thermal Resistance (R_t) (K/W)	0.0036	±1.85E-5	±0.51
Average Inner Wall Temperature (T_{wi}) ($°C$)	13.58	±0.5	±1.48
$T_{wi} - T_B$ (ΔT) ($°C$)	3	±1.01	±5.6
Heat Transfer Rate ($\dot{q}$) (W)	375.56	±5.30	±1.36
Heat Flux ($\dot{q}''$) (W/m^2)	9396.25	±156.8	±1.67
Heat Transfer Coefficient (h) ($W/m^2\text{-}K$)	2639.82	±921.75	±34.92

Table A-4 Uncertainty Calculations Best Case +20° (RUN 0093)

Variable	Value	Uncertainty	Uncertainty %
Inner Diameter (D_i) (m)	0.0125	±1.270E-05	±0.1
Outer Diameter (D_o) (m)	0.0171	±1.270E-05	±0.07
Length (L) (m)	1.016	±3.175E-03	0.31
Thermal Conductivity (k) ($W/m\text{-}K$)	13.438	NA	NA
Ampere (i) (A)	516.29	±5.16	±1.00
Voltage (V_D) (V)	3.54	±0.0354	±1.00
Thermal Resistance (R_t) (K/W)	0.0036	±1.85E-5	±0.51
Average Inner Wall Temperature (T_{wi}) ($°C$)	29.68	±0.5	±1.48
$T_{wi} - T_B$ (ΔT) ($°C$)	9	±1.01	±11
Heat Transfer Rate ($\dot{q}$) (W)	375.56	±25.87	±1.36
Heat Flux ($\dot{q}''$) (W/m^2)	45705.48	±764.24	±1.67
Heat Transfer Coefficient (h) ($W/m^2\text{-}K$)	5102.54	±540.75	±10.59

VITA

SRINAGA BHARATH CHANDRA

Candidate for the Degree of

Master of Science

Thesis: NON-BOILING HEAT TRANSFER IN HORIZONTAL AND NEAR HORIZONTAL UPWARD INCLINED GAS-LIQUID TWO PHASE FLOW.

Major Field: Mechanical and Aerospace Engineering

Biographical:

Education:

Completed the requirements for the Master of Sciences in Mechanical Engineering at Oklahoma State University, Stillwater, Oklahoma in July, 2014.

Completed the requirements for the Bachelor of Technology in Mechanical Engineering at DVR College of Engineering and Technology, JNTU, Hyderabad, Andhra Pradesh, India in 2012.

Experience: Graduate Teaching and Research Assistant in Oklahoma State University, Stillwater from 2012-2014.

Professional Memberships: ASME.